Project T10022: The combined effects of aneugenic benzimidazoles and other aneugens which act by disrupting microtubuli assembly

Final Report

May 2012

Dr Sibylle Ermler
Martin Scholze
Prof Andreas Kortenkamp
Institute for the Environment,
Brunel University

Project title
The combined effects of aneugenic benzimidazoles and other aneugens which act by disrupting microtubuli assembly

Project number
T010022

Aims of project
- To implement and validate automated micronucleus scoring by image analysis technologies
- To conduct dose-response analyses with benzimidazoles and non-benzimidazoles in the *in vitro* micronucleus assay
- To assess whether combinations of benzimidazoles that disrupt tubulin assembly induce micronuclei following the dose addition principle
- To evaluate whether mixtures of benzimidazoles and non-benzimidazoles capable of inducing micronuclei act in a dose-additive fashion

Start date
June 2010

End date
May 2012

Executive Summary

Benzimidazoles are used as fungicides and anthelmintics. Many of these chemicals are well recognised aneugens, capable of disrupting microtubule assembly through binding to tubulin subunits. This process can lead to the formation of micronuclei (MN). Considering this similarity in mechanism it is likely that several benzimidazoles might work together to induce MN according to the principles of concentration addition (CA). If that is the case, benzimidazoles could be grouped together for the purpose of cumulative risk assessment, with inhibition of tubulin polymerisation as the grouping criterion. However, empirical evidence of combination effects of benzimidazoles is missing altogether. This knowledge gap was highlighted in a 2007 report of the UK Committee on Mutagenicity of Chemicals (COM 2007). The committee made detailed research recommendations to fill this gap.

The present project was drawn up to respond to the COM (2007) recommendations. Its primary aim was to test whether combinations of benzimidazoles that induce MN by disrupting tubulin polymerisation do so according to the principles of CA.

To realise this aim, it was necessary to define conditions where CA and the alternative assessment concept of independent action (IA) produced differing additivity predictions. It was clear that little would be gained in resolving the issue highlighted by COM if the data emanating from this project agreed with both CA and IA. Especially with mixtures composed of only two chemicals, the two concepts often yield additivity expectations that are quantitatively very similar. The necessary discrimination between CA and IA could therefore only be achieved by working with multi-component mixtures of benzimidazoles.

The *in vitro* MN assay with the Chinese Hamster Ovary cell line CHO-K1 was used to establish concentration-response relationships for albendazole, albendazole oxide, benomyl, carbendazim, flubendazole, mebendazole, oxibendazole. By conducting simulation studies on the basis of these data we were able to establish that combinations of seven benzimidazoles would yield CA and IA additivity expectations that differed sufficiently to be resolved experimentally. A mixture ratio in proportion to the threshold concentrations of each benzimidazole for MN induction was chosen. Experimental assessment of this mixture revealed clear agreement with CA. At total mixture concentrations where each of the seven benzimidazoles was present at or below its threshold level, statistically significant mixture effects were observed. According to the principles of IA, this was not expected; the joint effects should have been similar to untreated control background levels.

These are the first data on combination effects of benzimidazole with MN formation as the endpoint. For the first time, we show conclusively that benzimidazoles act together according to the CA principles. Application of IA led to clear underestimations of the experimentally observed mixture effects.

A variety of non-benzimidazole aneugenic agents are also capable of disrupting microtubule formation, albeit by interacting with different binding sites. We investigated whether a mixture composed of such agents would also induce MN in a manner predictable by CA. The benzimidazole flubendazole was combined with the aneugens griseofulvin, colchicine, vinblastine and paclitaxel. Based on the concentration-response relationships for these chemicals, additivity expectations derived from CA and IA were calculated. As with the seven-component

benzimidazole mixture, these predictions differed sufficiently to be distinguished experimentally. For a mixture with a mixture ratio proportional to the individual threshold levels of each component, the observed combined effects fell slightly short of the CA prediction, but were higher than expected on the basis of IA. Flubendazole, colchicine and vinblastine all bind to the colchicine binding site of tubulin monomers thereby inhibiting microtubule polymerisation. Similarly, griseofulvin blocks the polymerisation of microtubule but binds to a different tubulin domain. Paclitaxel has yet another binding site and inhibits the depolymerisation of microtubules. Taking this into account, we employed a combined CA and IA model, which indeed agreed well with the observed effects.

Finally, we combined various agents capable of inducing MN by a variety of molecular mechanisms. This did not only include aneugens, but also clastogens. The aneugenic benzimidazole flubendazole was combined with the clastogens mitomycin C, etoposide, melphalan and doxorubicin, again at a mixture ratio proportional to the threshold concentrations of all components for MN formation. At the two highest concentrations, the effects of this mixture agreed with the IA prediction. However, at lower concentrations, where according to IA effects were not expected to occur, the MN frequencies were significantly higher than background levels. Thus, although this mixture came closest to the effects anticipated by IA, the IA principle was not fully realised. These findings also suggested a situation more in line with a hybrid model of CA and IA. Using the combined CA and IA model again provided a good estimate for the observed effects.

Our results show clearly that combinations of benzimidazoles act as predicted by CA. Disruption of microtubule polymerisation by binding to the tubulin monomers is therefore a good criterion for grouping these chemicals together for the purposes of cumulative risk assessment. Our data provide a decisive answer to the issue raised by COM.

The project also shows that CA can be used as a concept for dealing with chemicals that induce MN by additional mechanisms. With non-benzimidazole aneugens, CA provides reasonable approximations of the observed combination effects.

Even with combinations of chemicals that cause MN by a multitude of mechanisms, including clastogenic agents, the principles of IA are not fully realised. This provides support for the notion that MN formation, regardless of commonalities in molecular mechanisms, can be used as a phenomenological criterion for the grouping of chemicals for cumulative risk assessment. Even though a hybrid model of CA and IA may describe the experimentally observed effects better than IA, CA gives reasonable approximations of the empirical data. CA therefore suggests itself as the basis for cumulative risk assessment methods for such combinations, mainly because the data requirements for dealing with mixture effects according to IA, and to hybrids of CA and IA are unrealistically high.

Table of Contents

Executive Summary II
Chapter 1: Report Introduction 1
Introduction 2
Structure of the report 3
Chapter 2: Implementation and Validation of Automated Micronucleus Scoring by Image Analysis 4
Summary 5
Introduction 6
Results and discussion: Implementation and validation of automated micronucleus scoring by image analysis 7
Automated micronucleus scoring 7
Conclusions 14
Chapter 3: Dose-response Analysis with Individual Benzimidazoles and Non-benzimidazoles . 15
Summary 16
Introduction 17
Results and discussion: Dose-response analysis with individual benzimidazoles and non-benzimidazoles 18
Cytotoxicity testing of benzimidazoles in the MTT assay 19
Concentration-response analysis of individual compounds in the CBMN assay 24
Conclusions 31
Chapter 4: Mixture Experimentation – Mixtures of Benzimidazoles and Combinations of Benzimidazoles and Non-benzimidazole Genotoxins 32
Summary 33
Introduction 34
Results and discussion: Mixture experimentation 35
Combined effects of seven benzimidazoles (Mixture I) 35
Combined effects of benzimidazole and non-benzimidazole genotoxins 37
Combined effects of benzimidazole and non-benzimidazole aneugens (mixture II) 37
Combined effects of a benzimidazole and non-benzimidazole clastogens (mixture III) 40
Combined effects of a benzimidazole and a non-benzimidazole aneugen (mixture IV) 43
Conclusions 47
Chapter 5: Discussion and Conclusions 49
Discussion and implications for cumulative risk assessment 50
Predictability of mixture effects of benzimidazoles 50
Combinations of flubendazole with other non-benzimidazole aneugens 51

Combinations of flubendazole with clastogens 52
Implications for grouping criteria 52
Chapter 6: Methodology 54
Chemicals and reagents 55
General cell culture 55
CBMN assay 55
Automated image acquisition and micronucleus scoring 56
MTT assay for cytotoxicity detection 56
Biostatistical analysis of the CBMN assay 57
Threshold dose-response models 58
Mixture predictions 59
Mixture experiment design and testing 63
References 65

Chapter 1:
Report Introduction

Introduction

This report presents the results and final conclusions from Project T10022, the assessment of "The combined effects of aneugenic benzimidazoles and other aneugens which act by disrupting microtubuli assembly".

The aim of Project T10022 was to test the hypothesis that combinations of benzimidazoles which act by disrupting microtubule assembly do so by following the dose addition principle. Clarification of this point was requested by the Committee on Mutagenicity of Chemicals (COM). It was suspected that benzimidazole pesticides with a common mode of action act together according to dose addition. However, experimental evidence to support this notion was missing, but urgently required before benzimidazoles could be grouped together and subjected to cumulative risk assessment.

The two competing prediction models of dose or concentration addition (DA or CA) and independent action (IA) often yield identical predictions of additive combination effects. Therefore, it was crucial to define experimental design conditions where CA and IA produce mixture effect predictions that can be distinguished experimentally.

The quantitative differences between the additivity expectations produced by either CA or IA depend on the mathematical features of either concept (Drescher and Boedeker 1995) and their magnitude is influenced by (a) the mixture ratio, (b) the steepness of the concentration-response curves of the mixture components, (c) the number of mixture components, and (d) the level of effect chosen for assessment. The steepness of concentration-response curves cannot be influenced, and there is relatively little scope for variation of the mixture ratio as it should be avoided that one mixture component contributes disproportionally to the mixture effect. Therefore, the number of mixture components is the crucial variable that determines whether the predictions derived from CA and IA can be discriminated experimentally.

Accordingly, it seemed highly unlikely, that studies with selected binary mixture would yield conclusive results as to which mixture prediction model applies to mixtures of benzimidazoles, multi-component mixture experiments with benzimidazoles were to be carried out. To this end, a set of benzimidazoles listed as positive to induce micronuclei (MN) by disruption of microtubuli by COM (2007) were chosen to be subjected to extensive concentration-response analysis in an *in vitro* MN assay with the aim of including them in a multi-component mixture.

To be able to produce and manage the required amount of concentration-response data necessary for conducting such multi-component mixture studies a suitable *in vitro* MN assay system had to be chosen and an automated MN scoring system using image analysis to be implemented.

Structure of the report

Project T10022 had five research objectives:

1. To implement and validate automated micronucleus scoring by image analysis technologies
2. To conduct dose-response analyses with benzimidazoles and non-benzimidazoles in the in vitro micronucleus assay
3. To assess whether combinations of benzimidazoles that disrupt tubulin assembly induce micronuclei following the dose addition principle
4. To evaluate whether mixtures of benzimidazoles and non-benzimidazoles capable of inducing micronuclei act in a dose-additive fashion
5. To prepare a final report and scientific papers arising from the work

The chapters (2 – 4) of the report are structured along the objectives one to four, which also reflect the four tasks of the project. Research objective 5 is this report and scientific publications are currently under preparation.

For each task, a short introduction is given and the results are presented. Detailed descriptions of method development are given in the respective results chapters. General methodologies used in this project are described at the end of the report in Chapter 6.

Chapter 5 discusses the project's findings and their implications for the risk assessment of mixtures of benzimidazoles.

Chapter 2:
Implementation and Validation of Automated Micronucleus Scoring by Image Analysis

Task 1

Summary

Task 1 of Project T10022 comprised the method development in preparation for the work to be conducted in project **Tasks 2 to 4.**

In summary:

- An *in vitro* micronucleus assay using CHO-K1 cells has been established and optimised. The cytokinesis blocked micronucleus (CBMN) assay protocol was adapted to the requirements of automated imaging and analysis using a fluorescence microscope.
- An automated system for MN scoring by image analysis was implemented and validated for the CBMN assay using CHO-K1 cells.
- Assay procedures and automated MN scoring algorithms were optimised for the generation of high quality concentration-response data in the following tasks.

Introduction

Task 1 of project T10022 comprised the implementation and validation of the assay protocol for the cytokinesis blocked micronucleus (CBMN) assay followed by automated micronucleus scoring by image analysis.

This chapter covers the implementation and optimisation of sample preparation and staining procedures that were required to obtain samples suitable for automated image acquisition and subsequent micronucleus analysis. The cells employed for conducting the CBMN assay are the Chinese hamster ovary derived cell line CHO-K1 (ATCC), which is well established for micronucleus scoring, with high sensitivity for clastogenic and aneugenic chemicals. The assay protocol for the CBMN assay has been optimised to meet the requirements for automated image analysis with regard to treatment times, cell densities, sample preparation and staining procedures.

An overview about the automated imaging and analysis system employed for these analyses is also presented. The imaging system used for acquisition of microscopic images, followed by automated image analysis to score micronuclei (MN) is the Pathfinder™ Cellscan µN platform (IMSTAR, France).

Results and discussion:
Implementation and validation of automated micronucleus scoring by image analysis

The aim of task 1 of the project was to implement and validate an automated method for acquisition of microscopic images, followed by automated image analysis to score micronuclei (MN). The imaging system used for this project is the Pathfinder™ Cellscan µN platform which was purchased from IMSTAR (France). Setup and comprehensive training on the system was conducted by a representative from IMSTAR and all protocol developments and optimizations were carried out in close cooperation with the company.

Automated micronucleus scoring

To allow for automated micronucleus scoring, first the preparation and staining procedures for the cells needed to be established and optimised.

The CHO-K1 (Chinese hamster ovary) cell line was chosen for the analysis, as this is a well established cell line for micronucleus scoring, with high sensitivity for clastogenic and aneugenic chemicals. Other cell lines such as human lymphocytes were taken into consideration as well, but due to the commercial availability of CHO-K1 cells (American Type Culture Collection, ATCC) and their recognition as standard cell line for the type of studies conducted in this project, we decided to use the CHO-K1 cells.

Optimisation of cell preparations for automated micronucleus scoring

The standard protocol for MN detection in our laboratory so far comprised the treatment of cells, grown on glass slides or coverslips, followed by staining with either Giemsa, for light microscopy, or DAPI for fluorescence microscopy.

The automated system for MN scoring employs a fluorescent microscope and the recommended staining procedure suggested the use of acridine orange (AO). AO is a fluorescent dye, which allows staining of both the nuclei and cytoplasm of a cell. If bound to DNA it emits green light and under the more acidic conditions of the cytoplasm it emits orange light. Both, detection of cells and the nuclei within are required for the automated MN scoring. To provide an appropriate quality of samples, fulfilling the requirements for automated imaging and analysis, the optimisation of the cell preparation protocol was carried out in close cooperation with IMSTAR.

To ensure that the treatment did not inhibit cell proliferation and the cells had undergone at least one division before MN were analysed, a cytokinesis block with cytochalasin B was carried out. This allowed the nuclei to undergo division, but blocked the cell itself from dividing, thus leading to binucleated cells, which were used for MN scoring. An image of CHO-K1 cells grown on glass slides and stained after the cytochalasin B block is shown in Figure 1. The cells were stained with AO and the cytoplasm is shown in red and the nuclei in green. Almost all cells were binucleated, i.e. successfully blocked from cell division.

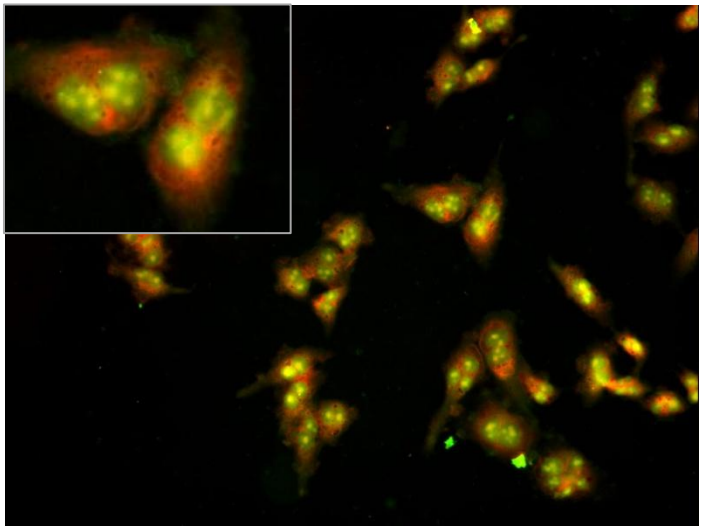

Figure 1: Binucleated CHO-K1 cells grown on slides, stained with AO. Cells were treated with cytochalasin B to block cytokinesis (CBMN assay). The AO staining shows cytoplasm in red and nuclei in green. The insert is a magnification of two cells to illustrate that each cell contains two nuclei.

During the implementation of the automated imaging system for MN scoring, it emerged that cells grown on slides were not suitable for automated analysis, as the formation of colonies prevented the individual cells from being accurately detected.

We made some attempts to fix, or fix and stain, cells in suspension before dropping them onto glass slides. However, the resulting preparations did not produce homogenous cell distributions across the slides and were thus not suitable for automated imaging.

To solve this problem, we purchased a cyto-centrifuge, which allowed the use of single cell suspensions which could be distributed evenly over a defined area of a glass slide.

Furthermore, the use of AO did not deliver staining of nuclei of a consistent quality required for the detection of binucleated cells containing micronuclei. Thus, we decided to use mounting medium containing DAPI for the staining of nuclei. DAPI staining consistently gave a good quality of nuclear staining.

A comparison of nuclear staining with AO (green channel) and DAPI in binucleated CHO-K1 cells is shown in Figure 2. A merged image of all 3 channels, including the cytoplasm in red is also shown. The images illustrate that in AO green (grey scale image of the green channel, left), the cytoplasm also exhibited green staining and for some preparations the difference between nuclei and cytoplasm was hardly distinguishable. DAPI staining (grey scale image of the blue channel, middle) on the other hand, always resulted in exclusive staining of the nuclei. Thus, DAPI was chosen as nuclear staining for all further preparations.

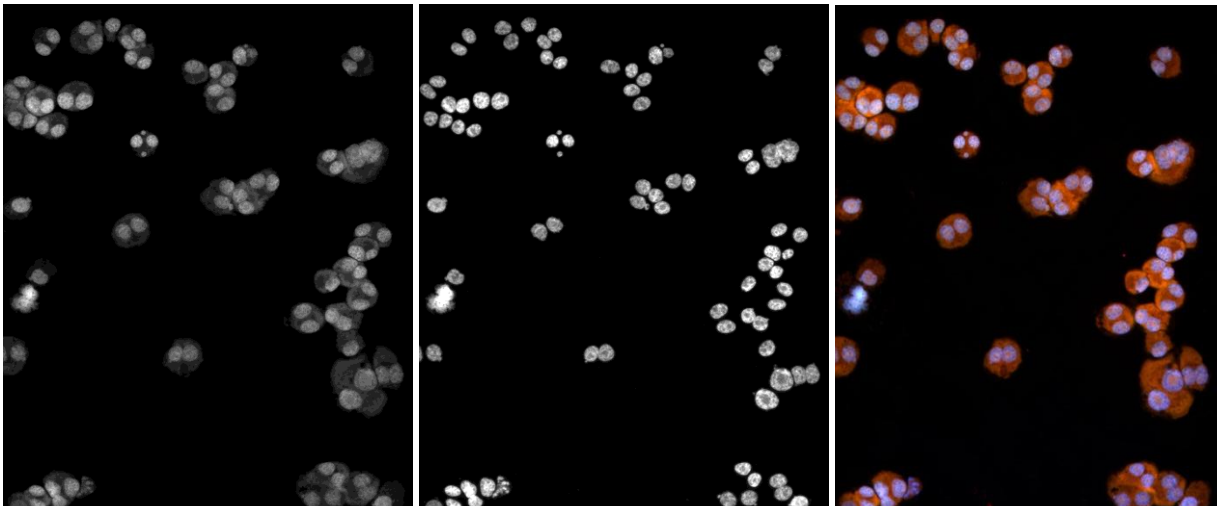

Figure 2: Comparison of nuclear staining with AO (left) and DAPI (middle) in binucleated CHO-K1 cells. The right image shows a merged image of the green (AO, nucleus), blue (DAPI, nucleus) and red channel (AO, cytoplasm).

For automated cell imaging, it is crucial to obtain a homogenous distribution of single cells across the glass slide. Several cell densities were tested from 1 x 10^6 cells down to 5,000 cells with various different inserts for the cyto-centrifuge. The use of 5,000 to 10,000 cells for the small inserts and 50,000 to 100,000 for large inserts turned out to be the most feasible cell number. It ensured that the cells were well spread over the slide whilst still resulting in enough cells for analysis. Decreasing the cell density to these lower cell numbers also allowed scaling down of the treatments from growing the cells in T25 flasks to 24 well plates. This further facilitated a more rapid treatment schedule with higher sample numbers and reductions in the amount of reagents required. An example for a slide containing CHO-K1 cells at an appropriate cell density is shown in Figure 3. It shows the nuclei of binucleated cells, which were treated with mitomycin C to induce MNs (red arrows).

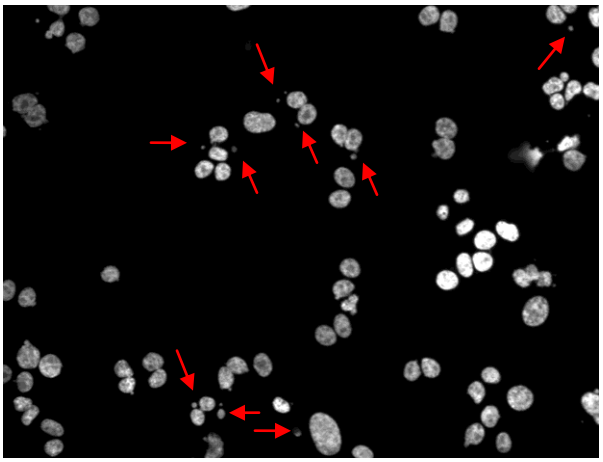

Figure 3: Binucleated CHO-K1 cells after cyto-centrifugation of 5,000 to 10,000 cells. The image shows the nuclear staining (DAPI) of binucleated cells. Cells were treated with mitomycin C to induce MNs (red arrows).

Automated image acquisition

The Pathfinder™ Cellscan µN platform can process up to four slides per automated image acquisition step. A suitably sized field needs to be defined on each slide, which is then scanned by the system. It records a mosaic of images in the desired fluorescence channels (AO red and DAPI blue). Having established the appropriate cell densities and staining procedures for the slide preparations, slides were imaged with the automated imaging system.

An example for two such mosaics is shown in Figure 4. The upper two images show the DAPI (left) and AO red (right) mosaic of a sample containing cells at a too high a density. In the lower panel a sample containing an appropriate cell density is shown (left: DAPI, right AO red).

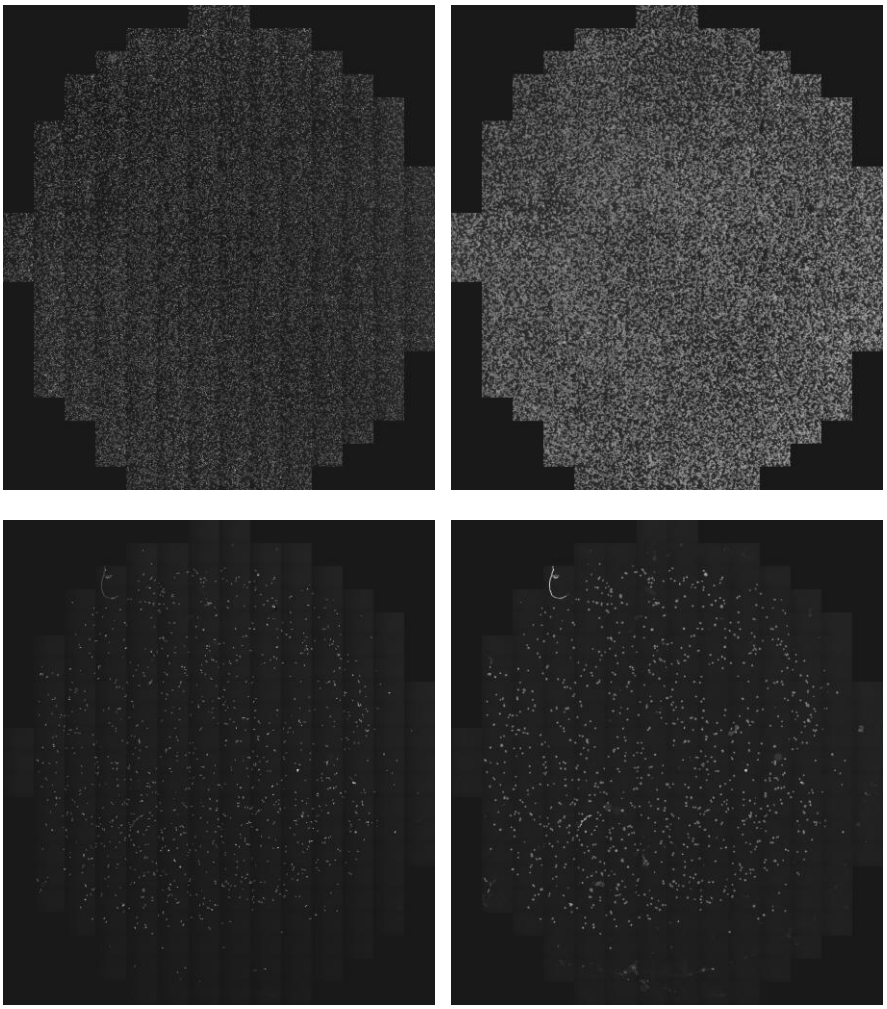

Figure 4: Example image mosaics after automated image acquisition. CHO-K1 cells were cytocentrifuged onto glass slides and stained with AO and DAPI. The upper panel shows the images for nuclear staining (DAPI, left) and cytoplasmic staining (AO red, right) of a sample with a high cell density. The lower panel shows the images for nuclear staining (DAPI, left) and cytoplasmic staining (AO red, right) of a sample at an appropriate cell density.

Automated micronucleus scoring

For automated MN scoring using the Pathfinder™ software, images of cells stained with AO and DAPI were captured and representative cells were marked and labelled. These images were sent to IMSTAR and used to develop the algorithms for image analysis.

Figure 5 illustrates how the cells were labelled. In the left image, the cytoplasmic staining (AO) is shown and two cells were marked as typical cells for the detection in the AO red channel. The same two cells are presented in the right picture, showing the nuclear stain (DAPI). Both cells are binucleated and contain MNs, which were marked on the image.

For training of the analysis software, a set of typical binucleated cells with and without micronuclei were submitted to IMSTAR. Mononucleated cells were labelled as well to allow discrimination between mono- and binucleated cells. This allowed for the possibility of using the ratio between mono- and binucleated cells as an additional measure for cytotoxicity.

In a first step, the software was trained to detect cells in the red channel. Next, the nuclei within the cells were detected, to facilitate analysis of only binucleated cells. After this step, the MNs within the detected mono- and binucleated cells were scored.

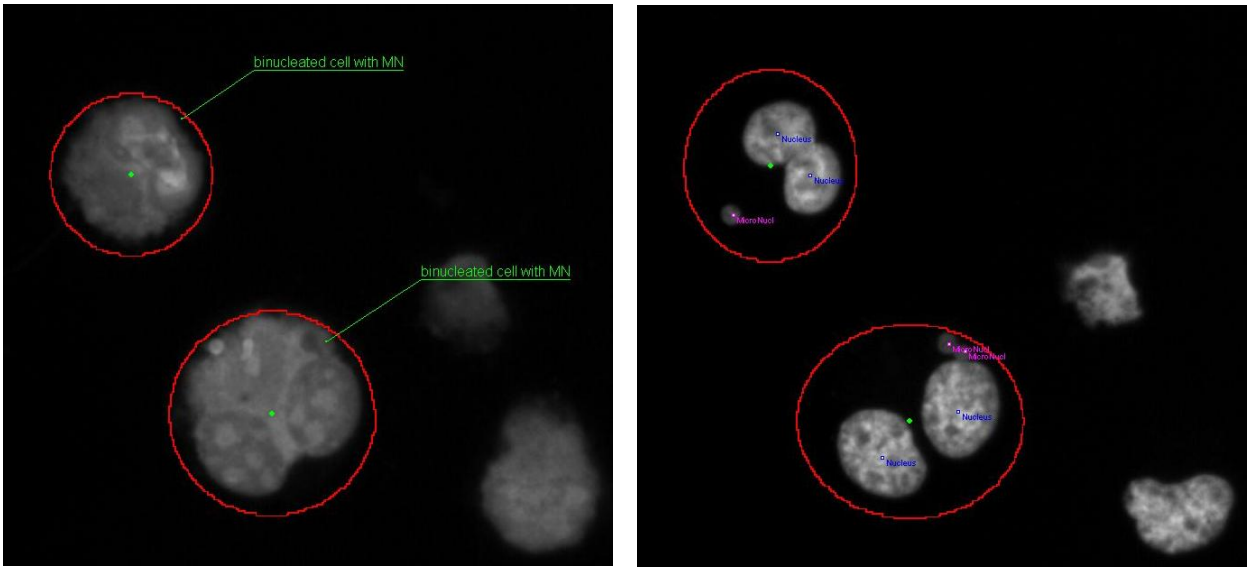

Figure 5: Labelling of binucleated CHO-K1 cells containing MNs for automated image analysis. CHO-K1 cells were treated with mitomycin C to induce MNs, followed by treatment with cytochalasin B to block cytokinesis (CBMN assay). Images of AO and DAPI stained cells were taken in the red (left) and blue channel (right). Cells were labelled using the cytoplasmic stain (left) and the nuclear staining was used to mark nuclei and MNs (right).
The green labels (left) mark "binucleated cells with MN". The blue and pink labels (right) mark "Nuclei" and "Micronuclei", respectively.

The algorithm developed in this way was installed in the imaging software and example slides were automatically analysed. To allow the verification of correct detection of nuclei and micronuclei, the software is equipped with a validation step (Figure 6). During validation, each detected object is shown and can be validated or rejected by the user. This step allowed for verification of the specific detection of cells, nuclei and MNs and the identification of false positives. Examples of false positives were identified (Figure 6) and sent to IMSTAR to refine the analysis algorithm. These false positives included detection of anaphase bridges, mitotic chromosomes, apoptotic cells and unspecific artefacts. Although the validation could in theory be carried out for each dataset, this is time consuming and was not deemed feasible in view of the amount of data required for our analysis. Therefore, the algorithm was optimised as well as possible and the amount of remaining false positives assumed to be equally distributed amongst the samples. It should also be noted that the validation step does not allow detection of false negatives. This is one of the reasons, why most of the automated analysis systems deliver overall lower MN scores than manual counts as has been described previously (Castelein et al. 1993, Varga et al. 2004, Decordier et al. 2008). Our own observations from comparisons of manual counts with automated analysis, which were initially carried out, confirmed these findings. The automated analysis persistently underscored the MN as compared to manual counts. This was similar for clastogens and aneugens, and at various concentrations. These findings can be explained by the fact that the algorithm has only one image at a given exposure for analysis, whereas during manual analysis it is easier to re-adjust focus and judge objects with higher or lower signal intensity and include them in the scoring. The automated analysis is designed to make more conservative decisions as to avoid false positive results. This omission of equivocal signals, however, inevitably leads to false negatives. During refinement of the algorithm it turned out to be more important to avoid detection of false positives. Thus, more focus was put on the visual inspection of the images collected for analysis than the direct comparison to manual counts. In general a high emphasis was given to avoiding the detection of false positive MN. Therefore, the stringent settings for the algorithm might have led to an underscoring of MN. This disregard of doubtful MNs was to be preferred to false positive detections of artefacts.

Most importantly, the automated image analysis allowed generation of highly reproducible concentration-response data for MN induction. This was of great importance in the context of this project, whereas absolute MN frequencies were not relevant.

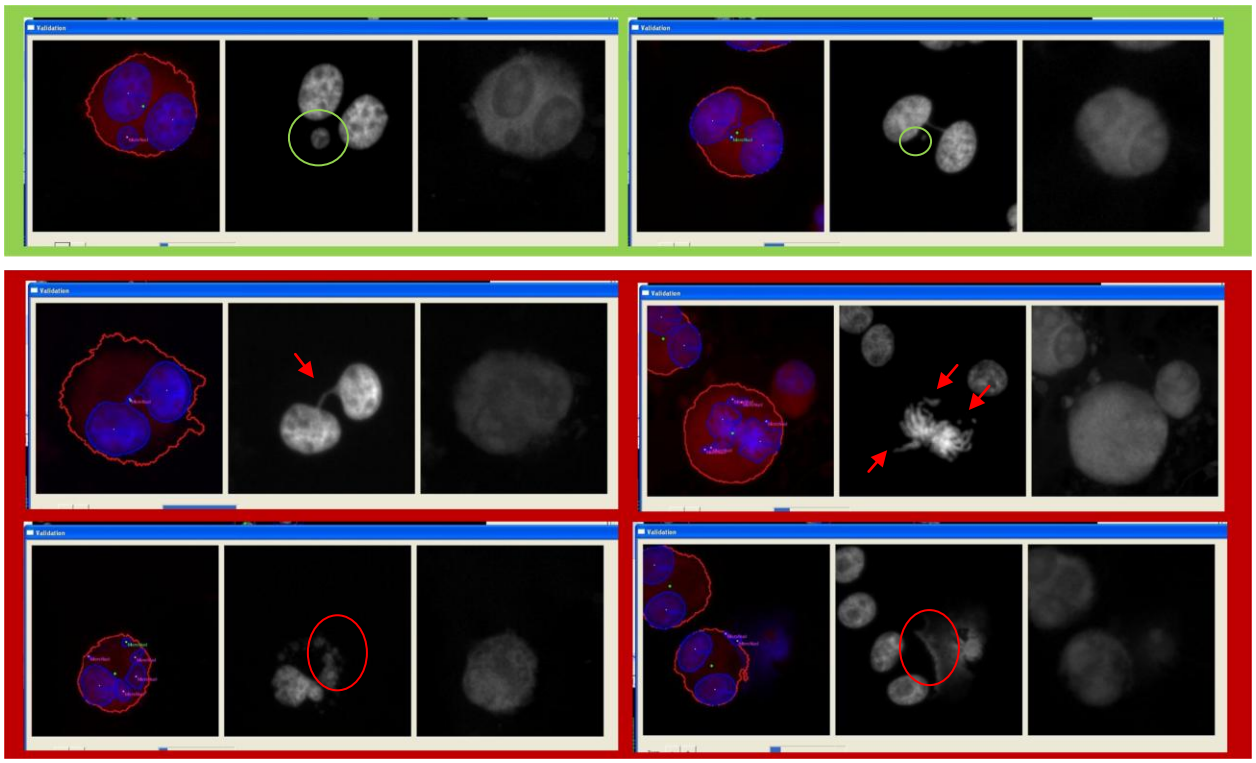

Figure 6: Screenshots from the validation of automated MN scoring.
Each screen shot shows an exemplary cell detected by the MN scoring algorithm. The colour image is the merged image from the DAPI and the Red channel plus the detected objects, in the middle is a grey scale image from the DAPI channel (nuclei) and on the right a greyscale image from the Red channel (cytoplasm). The upper panel (highlighted green) shows two examples of correctly scored micronuclei. The lower panels (highlighted red) show examples for false positive cells where either an anaphase bridge (middle left), a mitotic cell (middle right), an apoptotic cell (lower left) or unspecific stained material (lower right) was detected. The green circles in the DAPI channel indicate valid MNs, red arrows and circles show false positive detections of MNs.

Conclusions

Task 1 of Project T10022 comprised the implementation and validation of automated micronucleus scoring by image analysis. Work on this task included the establishment of a suitable assay protocol for an *in vitro* micronucleus test for automated analysis and the set up of the imaging and analysis system.

- An *in vitro* micronucleus assay using CHO-K1 cells has been established and optimised. The protocol uses a cytokinesis block following the treatments to assure that only cells that have completed one cell division are scored (CBMN assay). Sample preparation procedures included a cyto-centrifugation step to ensure cell separation and the cells were stained with fluorescent dyes for cytoplasm and nuclei to facilitate automated imaging and analysis using a fluorescence microscope.

- The automated imaging and MN scoring system by IMSTAR was implemented and validated for the CBMN assay using CHO-K1 cells. Automated scoring generally underscored the MN as compared to manual counts, but delivered reproducible concentration-response data for MN induction. Underscoring was expected and acceptable, as more emphasis was given to avoiding false positive counts and high data reproducibility. The MN scoring algorithm underwent several optimisation steps until the best possible results were achieved.

Chapter 3:
Dose-response Analysis with Individual Benzimidazoles and Non-benzimidazoles

Tasks 2 and 4

Summary

For **Tasks 2 and 4** of Project T10022 detailed concentration-response analysis of individual compounds were conducted in the CBMN assay. These comprised benzimidazole pesticides and additional, non-benzimidazole aneugens and clastogens. Further, the cytotoxicity for all test compounds was assessed in the MTT assay.

In summary we found that:

- Seven out of eight benzimidazoles, four out of five clastogens as well as all tested non-benzimidazole aneugens induced MNs in the CBMN assay using CHO-K1 cells.
- All effective compounds produced monotonic and nonlinear concentration-response relationships in the CBMN assay with no detectable cytotoxicity at low effect concentrations.
- A minimum of three independent experiments per individual compound were sufficient to accurately estimate their concentration-response relationships. All 15 test compounds produced highly reproducible data in the CBMN assay.
- Statistical analysis of the benzimidazole concentration-response suggested the inclusion of a threshold parameter in the regression modelling. This model assumption was expanded to all compounds and mixtures and taken into account in CA and IA predictions of the mixture effects.
- Cytotoxicity, as assessed in the MTT assay, did not affect the data quality of the CBMN assay (data variation, reproducibility) at concentrations below 40% cytotoxicity. Thus, only data from concentrations below the MTT-IC_{40} were included in the regression modelling and mixture effect predictions.
- All 15 compounds were considered as appropriate for inclusion in mixture studies.

Introduction

In this chapter, we present the concentration-response analysis data for all individual MN inducing compounds, benzimidazoles and non-benzimidazoles, which were subsequently included in mixture studies.

Whereas benzimidazoles all have the same mechanisms of action (MOA) in inducing MNs, we have chosen the additional aneugens to reflect a broader range of MOAs and have also decided to include some clastogens to be able to create an even more diverse mixture.

The benzimidazole pesticides included were the anthelmintics albendazole, its metabolite albendazole oxide, flubendazole, mebendazole and oxibendazole as well as the fungicides benomyl and its metabolite carbendazim, and thiabendazole which is used as both anthelmintic and fungicide. They all act by binding to the colchicine binding site of tubulin, thereby inhibiting microtubule formation, leading to the formation of MNs by loss of chromosomes.

The non-benzimidazole aneugens included in the studies were the anticancer drugs colchicine and vinblastine. These act in a way similar to the benzimidazoles. Also included was paclitaxel, which has a different tubulin binding site and leads to MN formation by microtubule stabilisation. We also chose the antifungal drug griseofulvin which has several tubulin binding sites thereby disrupting the proper functioning of microtubules. Clastogens lead to MNs by induction of DNA strand breaks, which can be formed by various MOAs. We tested mitomycin C, a cytotoxic antibiotic which leads to DNA crosslinks via alkylation. Melphalan was included, which is capable of alkylating DNA, albeit at different target sites than mitomycin C. Etoposide is a topoisomerase II inhibitor which causes DNA strand breaks by preventing the re-ligation of DNA strands during replication. Doxorubicin interacts with DNA by intercalation, also leading to loss of genetic material, similar to benzo(α)pyrene, which however requires metabolic activation.

All compounds were tested in the CBMN assay for induction of MNs and in the MTT assay to assess their cytotoxicity. The MTT assay was conducted to define a suitable concentration range where the results from MN scoring were not negatively influenced by cytotoxicity. Chemicals that produced MNs in a concentration dependent manner at concentrations suitably below the cytotoxicity range were subjected to detailed concentration-response analysis.

Results and discussion:
Dose-response analysis with individual benzimidazoles and non-benzimidazoles

In **Task 2**, concentration-response analyses with individual benzimidazoles were conducted in the CBMN assay, including the assessment of cytotoxicity for each compound in the MTT assay. This produced the concentration-response data for benzimidazoles that were essential to proceed with the mixture testing to be carried out in **Task 3**. **Task 4** was to test mixtures of benzimidazoles and non-benzimidazole aneugens, and we decided to also include clastogenic chemicals in the mixture testing. The results from the testing of these compounds in the CBMN and MTT assays are also presented in this chapter. The list of all benzimidazoles tested in the CBMN and MTT assays with their mode of action (MOA) and their activity in the CBMN assay is shown in Table 1, non-benzimidazole compounds are listed in Table 2.

The results from the MTT and CBMN assays are shown in the following paragraphs.

Table 1: Benzimidazoles tested in the CBMN assay and analysed by automated image analysis.
MOA (mode of action) indicated whether the compounds act as clastogens or aneugens.
CBMN activity indicates whether the chemical was active in the CBMN assay at the tested concentrations.

Compound	CAS#	MOA	CBMN activity
Albendazole	54965-21-8	aneugen	Yes
Albendazole oxide	54029-12-8	aneugen	Yes
Benomyl	17804-35-2	aneugen	Yes
Carbendazim	10605-21-7	aneugen	Yes
Flubendazole	31430-15-6	aneugen	Yes
Mebendazole	31431-39-7	aneugen	Yes
Oxibendazole	20559-55-1	aneugen	Yes
Thiabendazole	148-79-8	aneugen	No

Table 2: Non-benzimidazole aneugens and clastogens tested in the CBMN assay.
MOA (mode of action) indicated whether the compounds act as clastogen or aneugen.
CBMN activity indicates whether the chemical was active in the CBMN assay at the tested concentrations.

Compound	CAS#	MOA	CBMN activity
Colchicine	64-86-8	aneugen	Yes
Griseofulvin	126-07-8	aneugen	Yes
Vinblastine sulfate	143-67-9	aneugen	Yes
Paclitaxel	33069-62-4	aneugen	Yes
Mitomycin C	50-07-7	clastogen	Yes
Etoposide	33419-42-0	clastogen	Yes
Melphalan	148-82-3	clastogen	Yes
Doxorubicin hydrochloride	25316-40-9	clastogen	Yes
Benzo(α) pyrene	50-32-8	clastogen	No

Cytotoxicity testing of benzimidazoles in the MTT assay

Cytotoxicity testing (MTT) was carried out in CHO-K1 cells to define the concentration range for each benzimidazole to be tested in the CBMN (cytokinesis blocked micronucleus) assay. This ensured that cytotoxic effects of the compounds did not interfere with the results of the MN scoring (**Task 2**). Cytotoxicity for the non-benzimidazole compounds was assessed in parallel to the CBMN assay where the concentration range finding was based on literature data (**Task 4**).

All compounds were dissolved in DMSO as the solubility of the benzimidazoles in other solvents such as EtOH was too low to allow testing of sufficiently high concentrations. For most benzimidazoles, crystals formed at the highest tested concentrations in the cell culture medium, due to their low aqueous solubility.

The results of the cytotoxicity testing for the eight benzimidazole pesticides are shown in Figure 7. All benzimidazoles, except thiabendazole, were cytotoxic above a certain concentration. It was not possible to construct complete concentration-response curves for all compounds, as their low aqueous solubility prohibited the testing of higher concentrations.

However, the MTT data was adequate to define the concentration ranges for the benzimidazoles to be tested in the CBMN assay. Initially, cytotoxicity was limited to the MTT-IC_{20} of each compound, but was later relaxed to 40-50% cytotoxicity as within the stringent limitations only a few compounds produced MNs.

In the course of **Task 4** several additional non-benzimidazole aneugens and clastogens were tested in the CBMN assay. The MN inducing compounds were also tested in the MTT assay and the results from cytotoxicity testing are shown in Figure 8. The MN positive aneugens that were tested were colchicine, griseofulvin, paclitaxel and vinblastine, all of which induced up to 50% cytotoxicity in the tested concentration range. The clastogens doxorubicin, etoposide, melphalan and mitomycin C also showed some cytotoxicity at the highest concentrations.

The regression model and parameters, including the IC_{10}, IC_{20} and IC_{40} values for each compound are shown in Table 3.

Figure 7 (page 20):
Cytotoxicity of eight benzimidazoles.
All compounds were tested for cytotoxicity in the MTT assay using CHO-K1 cells. The graphs show the concentration-response data for cytotoxicity (black dots) for each compound (as indicated). The red curves show the respective regression curves with their 95% confidence intervals (dashed red lines). The box and whisker plots show the positive and negative controls at zero and one respectively. All benzimidazoles were tested in at least three independent experiments.

Figure 8 (page 21):
Cytotoxicity of non-benzimidazole aneugens and clastogens in the MTT assay.
All compounds were tested for cytotoxicity in the MTT assay using CHO-K1 cells. Colchicine, griseofulvin, paclitaxel and vinblastine are aneugens; doxorubicin, etoposide, melphalan and mitomycin C are clastogens. The graphs show the concentration-response data for cytotoxicity (black dots) for each compound (as indicated). Red curves show the respective regression curves with their 95% confidence intervals (dashed red lines). The box and whisker plots show the positive and negative controls at zero and one respectively. All compounds were tested in at least two independent experiments.

Albendazole

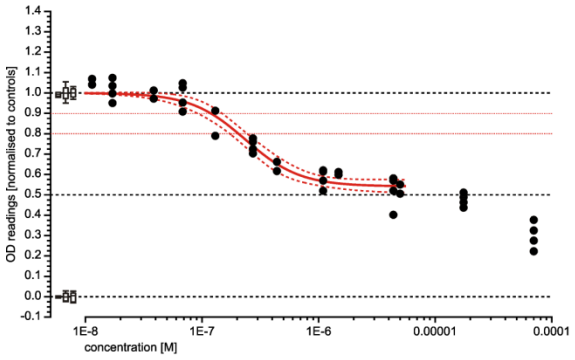

Albendazole oxide

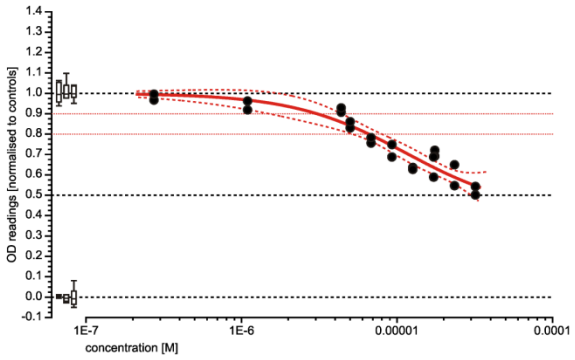

Benomyl

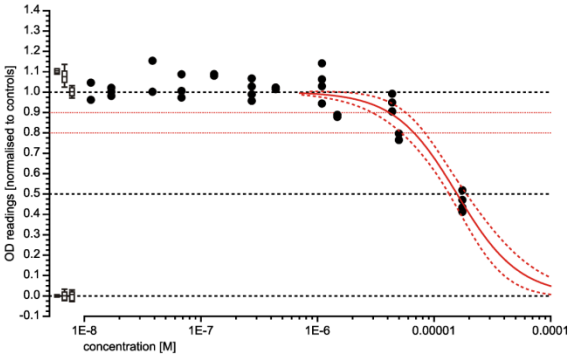

Carbendazim

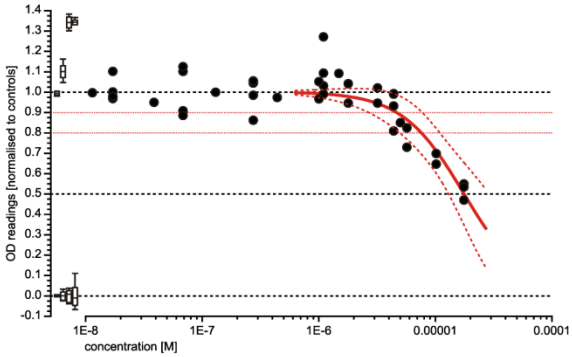

Flubendazole

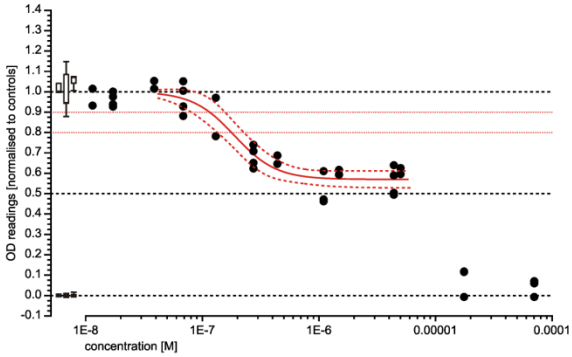

Mebendazole

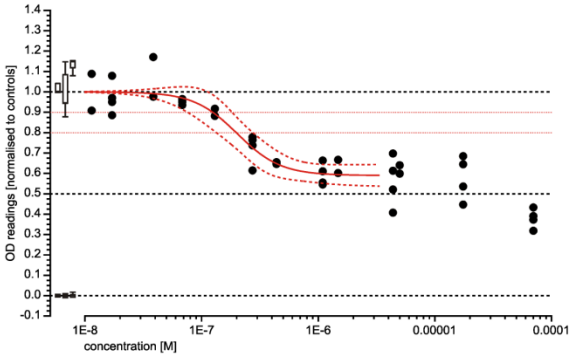

Oxibendazole

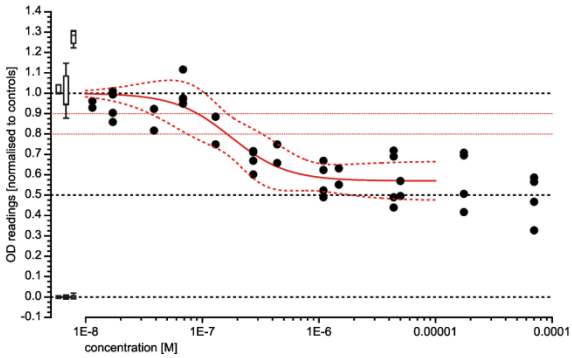

Thiabendazole

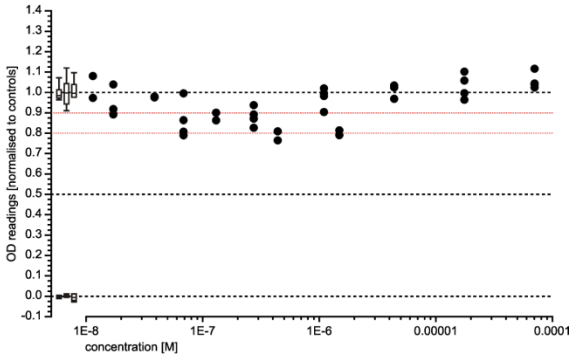

Colchicine

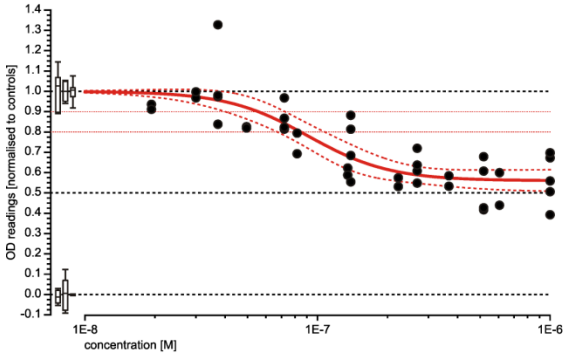

Griseofulvin

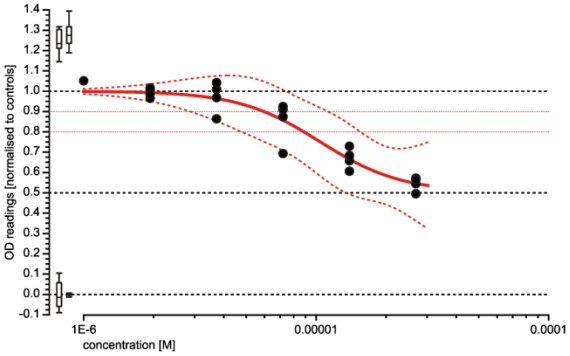

Paclitaxel

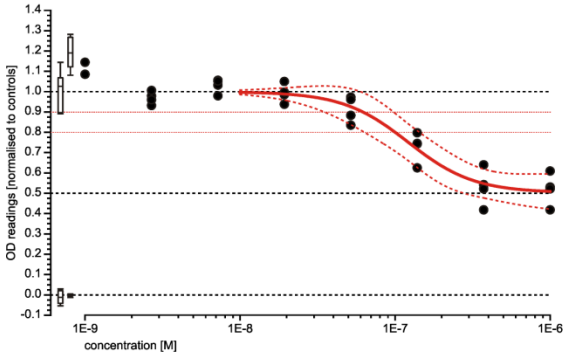

Vinblastine sulfate

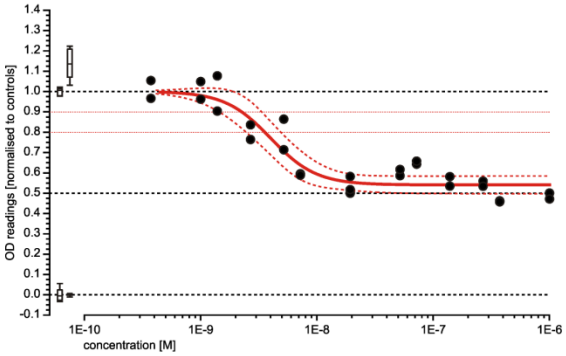

Doxorubicin hydrochloride

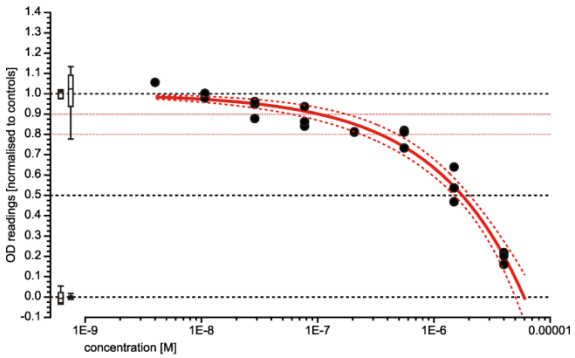

Etoposide

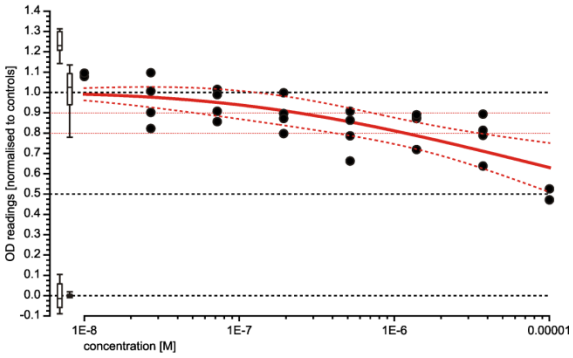

Melphalan

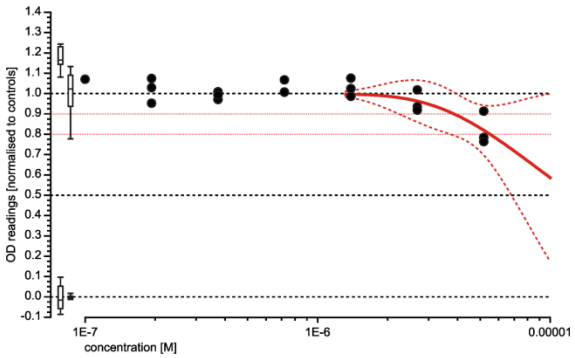

Mitomycin C

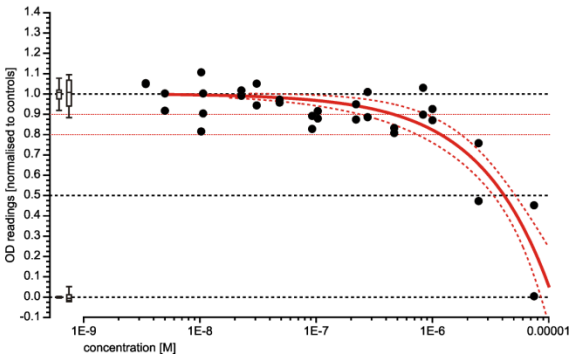

Table 3: Cytotoxicity of benzimidazoles and non-benzimidazoles in the MTT assay.

Substance	Concentration-Response Function						IC_{10}		IC_{20}		IC_{40}	
	RM	$\hat{\theta}_1$	$\hat{\theta}_2$	$\hat{\theta}_3$	$\hat{\theta}_{min}$	θ_{max}	M [CI]		M [CI]		M [CI]	
Aneugens (benzimidazoles)												
Albendazole	logit	-28.39	-4.28	--	0.54	1	1.19E-7	[9.29E-8 - 1.52E-7]	2.06E-7	[1.74E-7 - 2.43E-7]	6.63E-7	[4.76E-7 - 9.25E-7]
Benomyl	logit	-18.01	-3.75	--	0*	1	4.06E-6	[2.87E-6 - 5.76E-6]	6.69E-6	[5.27E-6 - 8.48E-6]	1.22E-5	[1.04E-5 - 1.43E-5]
Carbendazim	logit	-17.96	-3.78	--	0*	1	4.58E-6	[2.54E-6 - 8.26E-6]	7.51E-6	[5.05E-6 - 1.12E-5]	1.37E-5	[9.89E-6 - 1.89E-5]
Flubendazole	logit	-37.62	-5.59	--	0.57	1	1.15E-7	[8.03E-8 - 1.64E-7]	1.77E-7	[1.38E-7 - 2.28E-7]	5.44E-7	[3.03E-7 - 9.77E-7]
Mebendazole	logit	-35.89	-5.36	--	0.59	1	1.24E-7	[7.62E-8 - 2.03E-7]	1.98E-7	[1.42E-7 - 2.75E-7]	9.88E-7	[1.29E-7 - 7.54E-6]
Oxibendazole	logit	-49.89	-7.27	--	0.58	1	9.09E-8	[3.66E-8 - 2.26E-7]	1.63E-7	[9.67E-8 - 2.75E-7]	3.55E-7	[1.22E-7 - 1.03E-6]
Thiabendazole	-						>7E-5		>7E-5		>7E-5	
Albendazole Oxide	logit	-13.60	-2.75	--	0.41	1	3.03E-6	[1.78E-6 - 5.15E-6]	6.56E-6	[5.39E-6 - 7.98E-6]	2.16E-5	[1.75E-5 - 2.66E-5]
Aneugens (non-benzimidazole)												
Colchicine	logit	-40.12	-5.70	--	0.56	1	5.56E-8	[4.10E-8 - 7.55E-8]	8.47E-8	[6.78E-8 - 1.06E-7]	2.32E-7	[1.41E-7 - 3.84E-7]
Griseofulvin	logit	-28.44	-5.71	--	0.50	1	5.94E-6	[2.81E-6 - 1.25E-5]	8.83E-6	[5.22E-6 - 1.49E-5]	1.83E-5	[8.65E-6 - 3.88E-5]
Paclitaxel	logit	-32.66	-4.72	--	0.50	1	6.20E-8	[3.46E-8 - 1.11E-7]	1.00E-7	[6.84E-8 - 1.47E-7]	2.42E-7	[1.43E-7 - 4.11E-7]
Vinblastine sulfate	logit	-42.93	5.11	--	0.54	1	2.24E-9	[1.41E-9 - 3.58E-9]	3.55E-9	[2.54E-9 - 4.96E-9]	9.40E-9	[5.55E-9 - 1.59E-8]
Clastogens												
Doxorubicin hydrochloride	logit	8.59	-1.30	--	-483	1	1.01E-7	[5.79E-8 - 1.78E-7]	3.46E-7	[2.41E-7 - 4.96E-7]	1.18E-6	[9.78E-7 - 1.42E-6]
Etoposide	weibull	-2.58	-0.52	--	0*	1	2.32E-7	[5.76E-8 - 9.37E-7]	1.15E-6	[4.66E-7 - 2.86E-6]	1.44E-5	[2.77E-6 - 7.43E-5]
Melphalan	weibull	-11.73	-2.32	--	0*	1	3.88E-6	[2.46E-6 - 6.12E-6]	5.54E-6	[3.58E-6 - 8.56E-6]	>5.2E-6	
Mitomycin C	logit	-4.56	-1.69	--	45.22	1	4.53E-7	[2.29E-7 - 8.96E-7]	1.17E-6	[7.52E-7 - 1.82E-6]	3.03E-6	[2.38E-6 - 3.87E-6]

IC_{10}, IC_{20}, IC_{40}: concentrations provoking 10%, 20% and 40% lower OD readings to the negative controls, respectively. Values in brackets denote the upper and lower limits of the approximate 95% confidence interval; the column "RM" indicates the mathematical regression function as defined at Scholze *et al.* (2001): $\hat{\theta}_1, \hat{\theta}_2, \hat{\theta}_3, \hat{\theta}_{min}$ estimated model parameters, given for concentrations expressed in M (rounded values), θ_{max} were not estimated, but set to 1 relating to the mean value of the negative controls; * hold fixed; ">" indicates highest test concentration;

Concentration-response analysis of individual compounds in the CBMN assay

In **Task 2** concentration-response analyses of individual benzimidazoles were conducted in the CBMN assay and **Task 4** included the testing of additional, non-benzimidazole compounds.

We initially limited the testing of the compounds to concentrations associated with 20% cytotoxicity. This meant that some of the eight tested benzimidazoles (Table 1) lacked a response in the CBMN assay. We subsequently abandoned this restriction and tested all benzimidazoles up to their solubility limit in cell culture medium to examine whether they produced a response at all in the CBMN assay. After relaxing the cytotoxicity criterion, seven of the eight tested benzimidazoles were identified as inducing MNs in a concentration dependent manner. Thiabendazole had no effect in our assay system and was therefore excluded from further studies. The remaining seven positive benzimidazoles were subjected to detailed concentration-response analysis in the CBMN assay and the results for the individual compounds are shown in Figure 9 and Figure 10.

During the analysis of the CBMN data, we used the MTT assay results to define a new concentration limit up to which MN induction was reproducible with little variability. OECD guideline 487 states that concentrations that produce over 55 ± 5% cytotoxicity should not be considered for MN scoring. Therefore, we aimed not to exceed this value. In the end, a cytotoxicity value of 40% turned out to be a suitable cut off for excluding these concentrations from any mixture experimentation.

A typical concentration-response data set from the CBMN assay is shown for albendazole oxide in Figure 9: the dots show the data from four independent experiments (as indicated by different colours) and the grey areas indicate the concentration range where more than 40% cytotoxicity was observed in the MTT assay. The pooled data for the remaining benzimidazoles are shown in Figure 10, in each case derived from three or four independent experiments. In general, three experiments were sufficient. Only if the range finding experiment did not deliver enough data points within the effective range, the compound was tested a fourth time. For benzimidazoles that were tested in the cytotoxic (>IC_{40}) range data variability increased considerably due to the decreased number of analysable cells and the cytotoxic effects. Therefore, concentrations above 40% cytotoxicity were not included in the regression modelling.

As the detailed analysis of our results showed that the data was best represented by regression models including a threshold parameter, we assumed the threshold concept for the aneugenic effect of the benzimidazoles. As shown in Figure 9 and Figure 10, the cells carry a baseline percentage of MNs up to the threshold concentration above which the concentration dependent increase of MNs could be modelled by non linear regression models. Below our defined cytotoxic range, the intra- and inter-experimental data variability was acceptable and the assay delivered a good data reproducibility. All model parameters, as well as the baseline rate of MN induction and the threshold concentration for each compound are presented in Table 4. A detailed description of the biostatistical analysis of the CBMN data is included in the methodology chapter (Chapter 6).

Our empirical findings agree well with earlier reports of effect thresholds for spindle poisons (COT/COM/COC 1993, Elhajouji et al. 2011), in line with the hypothesis that a critical number of tubulin binding sites have to be occupied before the aneugenic effect emerges. Thus, the

threshold estimates for the individual benzimidazoles were taken into account in the modelling of their combined effect.

For **Task 4** a set of additional, non-benzimidazole aneugens as well as clastogens (Table 2) were tested in the CBMN assay. The four aneugens colchicine, griseofulvin, paclitaxel and vinblastine all induced MN in a concentration dependent manner (Figure 11). Of the tested clastogens, doxorubicin, etoposide, melphalan and mitomycin C were positive (Figure 11). Only benzo(α)pyrene did not induce MN (data not shown). Benzo(α)pyrene requires metabolic activation for the release of the ultimately active intermediate. The lack of activity of this chemical in CHO-K1 cells suggests that they lack the enzymes necessary for metabolic activation.

For most of the aneugens and clastogens the concentration-response data were also best described by including a threshold model parameter in the regression analysis and therefore we analysed them statistically in the same way as the benzimidazoles (detailed in Chapter 6). All model parameters, as well as the baseline rate of MN induction and the threshold concentration for each compound are presented in Table 4.

The assumption of a threshold concentration not only for aneugens, but also for clastogens is in agreement with reports for other clastogenic chemicals (Lynch et al. 2003) as well as observations for other endpoints (Boobis et al. 2009).

Figure 9: Induction of MNs by albendazole oxide in the CBMN assay.
Concentration-response analysis was conducted in the CBMN assay using CHO-K1 cells. The activity in the assay is shown as percentage of MN positive binucleated (bn) cells. The graph shows the experimental data of four independent experiments (black, red, green and blue dots). The black line shows the regression curve with the 95% confidence interval (dashed black lines). The controls are solvent treated cells (dots on the left, colours correspond to the experiment). The red horizontal line shows the mean baseline MNs present in the cells. The vertical dashed red line shows the estimated threshold concentration for the aneugenic effect of the compound. The grey area shows the cytotoxic concentration range for the compound as determined in the MTT assay (cytotoxicity > 40%).

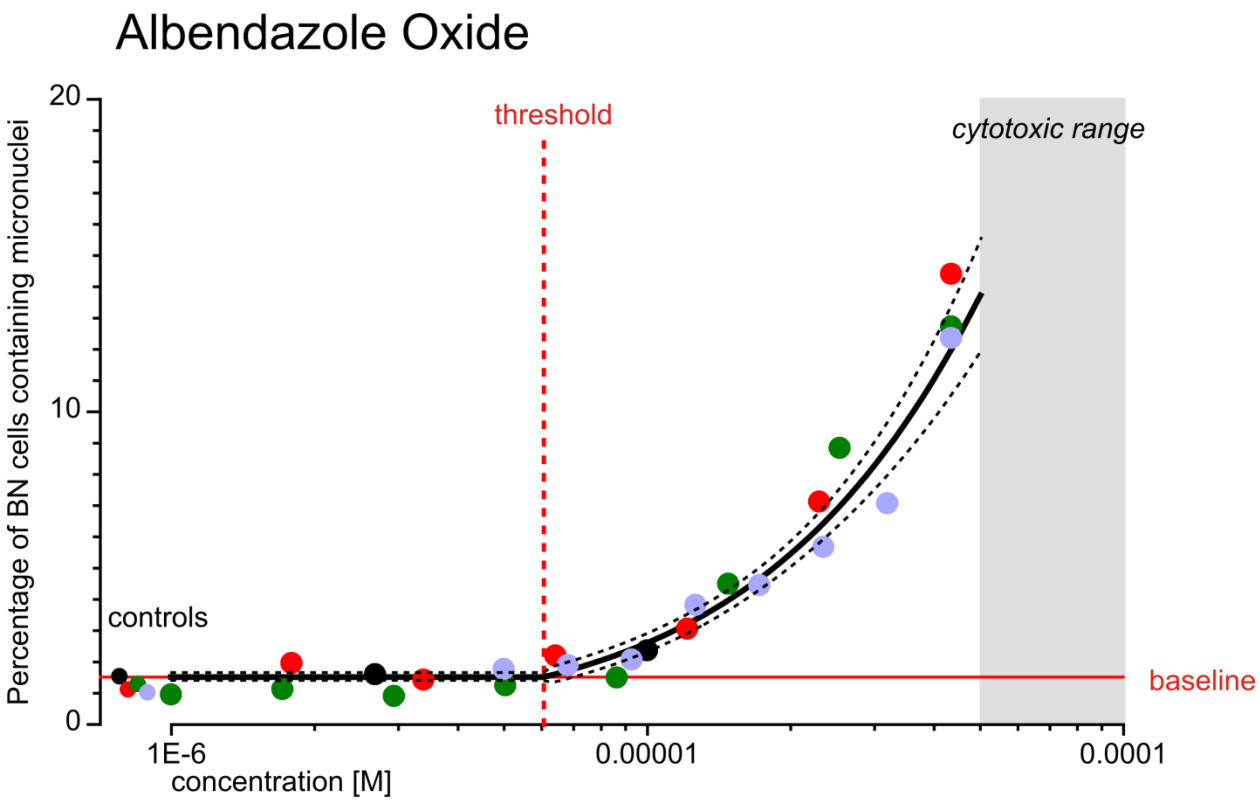

.

Figure 10 (page 27): Induction of MNs by six benzimidazoles in the CBMN assay.
Concentration-response analysis was conducted in the CBMN assay using CHO-K1 cells. The activity in the assay is shown as percentage of MN positive binucleated (bn) cells. The graph shows the pooled experimental data of three or four independent experiments (red dots). The black line shows the regression curve with the 95% confidence interval (dashed black lines). The controls are solvent treated cells (green dots, on the left). The red horizontal lines show the mean baseline MNs present in the cells. The vertical dashed red lines show the estimated threshold concentration for the aneugenic effect of the compounds. The grey area shows the cytotoxic concentration range for the compounds as determined in the MTT assay (cytotoxicity > 40%).

Figure 11 (page 28): Induction of MNs by non-benzimidazole aneugens and clastogens in the CBMN assay.
Concentration-response analysis was conducted in the CBMN assay using CHO-K1 cells. The activity in the assay is shown as percentage of MN positive binucleated (bn) cells. The graph shows the pooled experimental data of three or four independent experiments (red dots). The black line shows the regression curve with the 95% confidence interval (dashed black lines). The controls are solvent treated cells (green dots, on the left). The red horizontal lines show the mean baseline MNs present in the cells. The vertical dashed red lines show the estimated threshold concentration for the aneugenic or clastogenic effect of the compounds. The grey area shows the cytotoxic concentration range for the compounds as determined in the MTT assay (cytotoxicity > 40%).

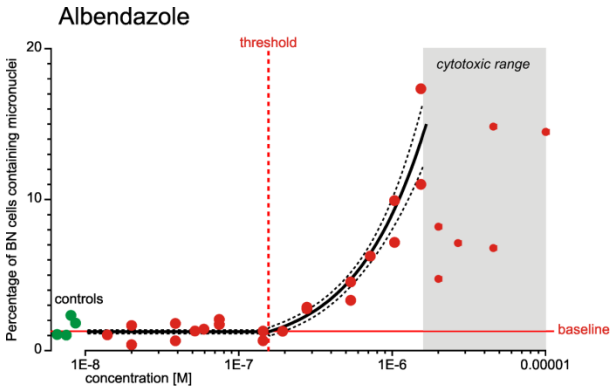
Albendazole
threshold
cytotoxic range
Percentage of BN cells containing micronuclei
20
10
0
controls
baseline
1E-8
1E-7
1E-6
0.00001
concentration [M]

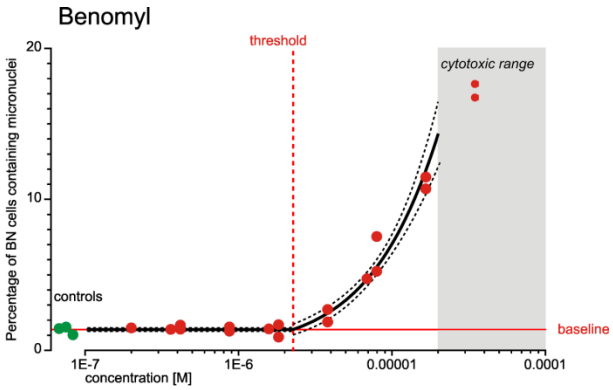
Benomyl
threshold
cytotoxic range
Percentage of BN cells containing micronuclei
20
10
0
controls
baseline
1E-7
1E-6
0.00001
0.0001
concentration [M]

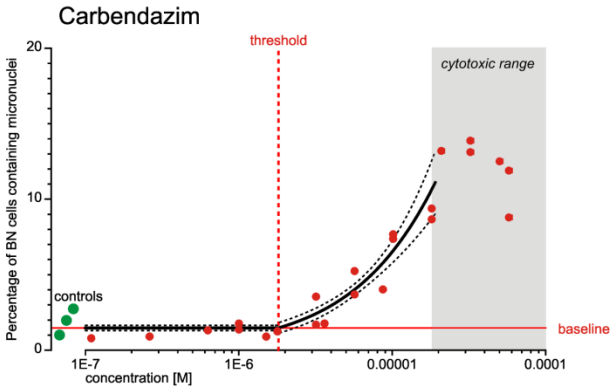
Carbendazim
threshold
cytotoxic range
Percentage of BN cells containing micronuclei
20
10
0
controls
baseline
1E-7
1E-6
0.00001
0.0001
concentration [M]

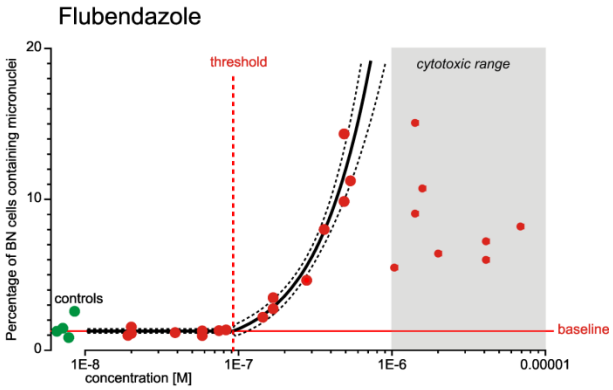
Flubendazole
threshold
cytotoxic range
Percentage of BN cells containing micronuclei
20
10
0
controls
baseline
1E-8
1E-7
1E-6
0.00001
concentration [M]

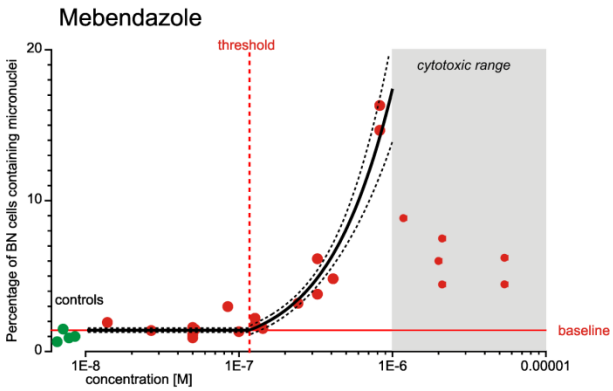
Mebendazole
threshold
cytotoxic range
Percentage of BN cells containing micronuclei
20
10
0
controls
baseline
1E-8
1E-7
1E-6
0.00001
concentration [M]

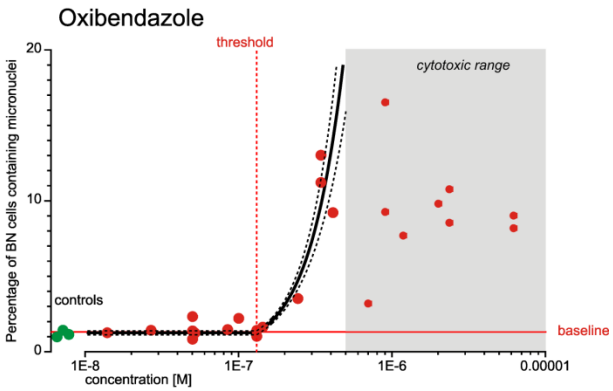
Oxibendazole
threshold
cytotoxic range
Percentage of BN cells containing micronuclei
20
10
0
controls
baseline
1E-8
1E-7
1E-6
0.00001
concentration [M]

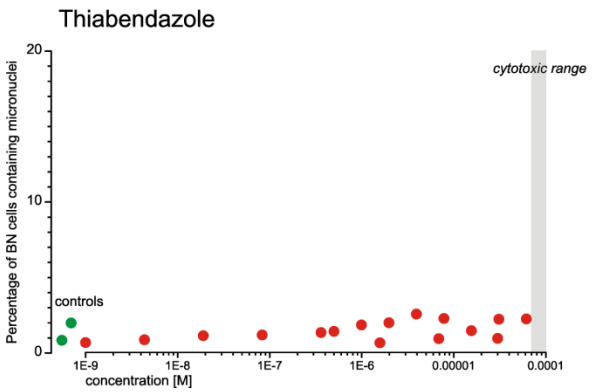
Thiabendazole
cytotoxic range
Percentage of BN cells containing micronuclei
20
10
0
controls
1E-9
1E-8
1E-7
1E-6
0.00001
0.0001
concentration [M]

Colchicine

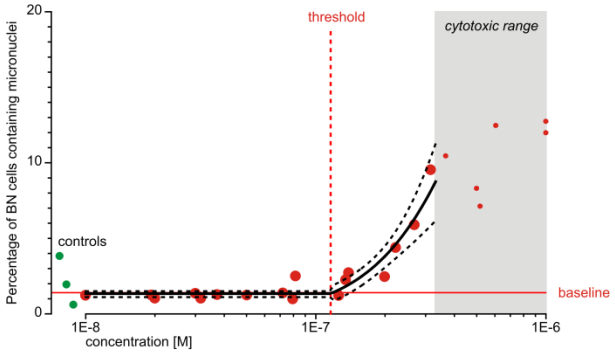

Griseofulvin

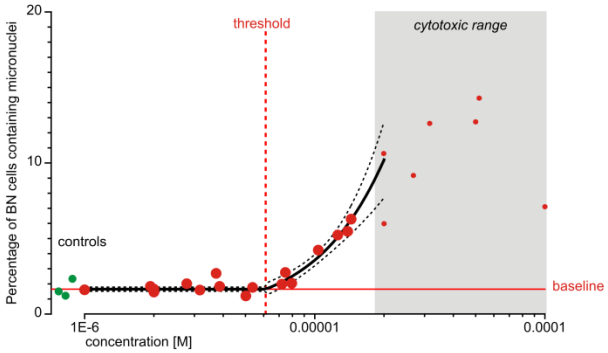

Paclitaxel

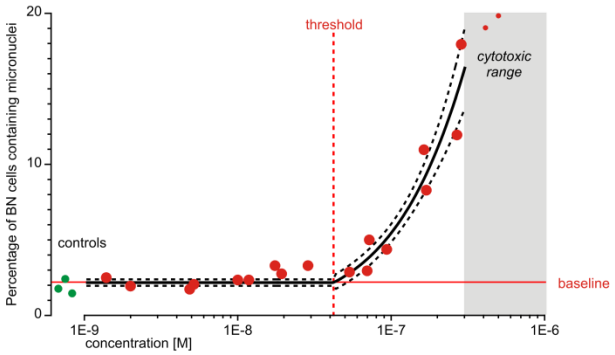

Vinblastine sulfate

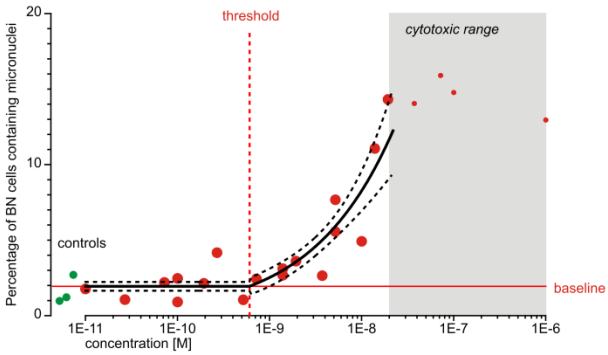

Doxorubicin hydrochloride

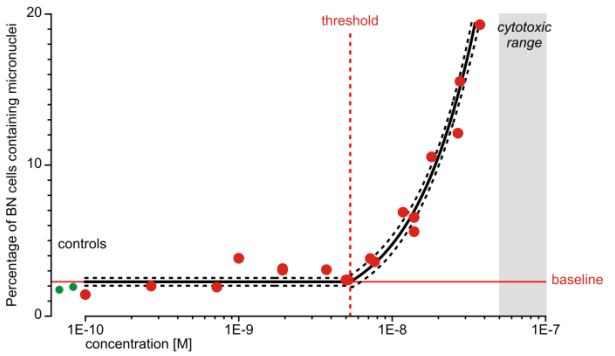

Etoposide

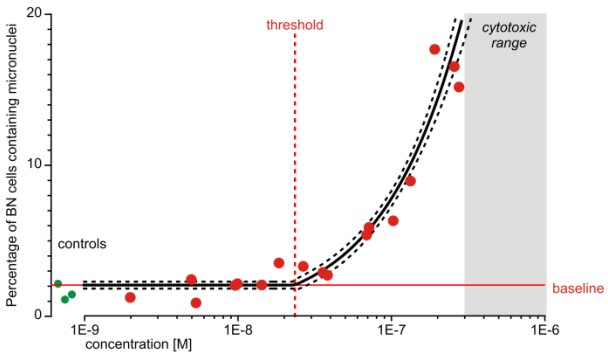

Melphalan

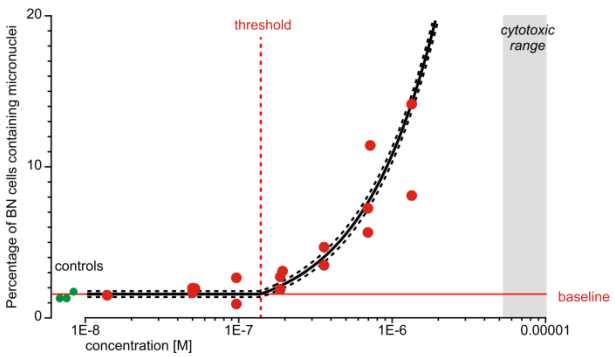

Mitomycin C

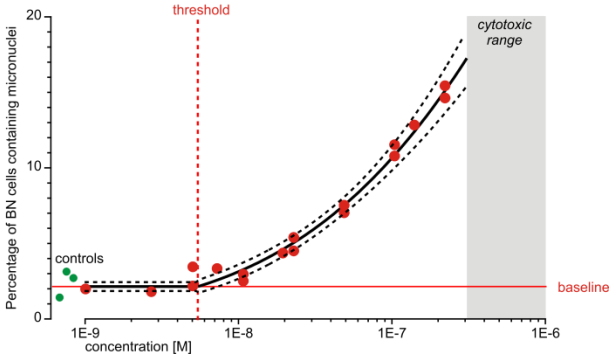

Table 4: Threshold concentration-response models for individual benzimidazoles and non-benzimidazoles in the CBMN assay.

Substance	model	model parameter $\hat{\theta}_1$	$\hat{\theta}_2$	$\hat{d}$	baseline rate* (95% CI)		threshold concentration (95%CI) [M]	
Aneugens (benzimidazoles)								
Albendazole	logit	-4.399	2.588	-6.807	1.21%	(1.09% -1.34%)	1.56E-07	(1.25E-07 -1.96E-07)
Benomyl	logit	-4.272	2.626	-5.644	1.38%	(1.27% -1.49%)	2.27E-06	(1.79E-06 -2.88E-06)
Carbendazim	logit	-4.213	2.085	-5.743	1.46%	(1.31% -1.61%)	1.81E-06	(1.40E-06 -2.34E-06)
Flubendazole	weibull	-4.358	3.134	-7.035	1.27%	(1.14% -1.41%)	9.22E-08	(7.29E-08 -1.16E-07)
Mebendazole	logit	-4.321	2.918	-6.950	1.31%	(1.18% -1.44%)	1.12E-07	(9.31E-08 -1.35E-07)
Oxibendazole	weibull	-4.378	5.004	-6.883	1.25%	(1.14% -1.35%)	1.31E-07	(1.31E-07 -1.32E-07)
Albendazole Oxide	logit	-4.168	2.543	-5.217	1.52%	(1.42% -1.63%)	6.07E-06	(5.24E-06 -7.04E-06)
Aneugens (non-benzimidazoles)								
Colchicine	probit	-2.228	1.903	-6.936	1.30%	(1.10%-1.49%)	1.16E-07	(9.50E-08-1.41E-07)
Vinblastine sulfate	weibull	-3.932	1.216	-9.219	1.94%	(1.65%-2.23%)	6.04E-10	(3.24E-10-1.12E-09)
Paclitaxel	logit	-3.810	2.549	-7.375	2.17%	(1.95%-2.38%)	4.22E-08	(3.37E-08-5.28E-08)
Griseofulvin	logit	-4.093	3.735	-5.213	1.64%	(1.45%-1.83%)	6.13E-06	(4.88E-06-7.69E-06)
Clastogens								
Melphalan	weibull	-4.149	2.307	-6.858	1.57%	(1.37%-1.76%)	1.39E-07	(1.16E-07-1.66E-07)
Doxorubicin hydrochloride	weibull	-3.778	2.756	-8.273	2.26%	(2.00%-2.52%)	5.33E-09	(4.42E-09-6.43E-09)
Etoposide	weibull	-3.872	2.156	-7.628	2.06%	(1.83%-2.29%)	2.36E-08	(1.88E-08-2.96E-08)
Mitomycin C	probit	-2.027	0.617	-8.268	2.14%	(1.84%-2.43%)	5.40E-09	(3.69E-09-7.88E-09)

* baseline rate is expressed as percentage; $\hat{\theta}_1, \hat{\theta}_2$ and $\hat{d}$ are estimates of the unknown model parameter θ_1, θ_2 and d.

Conclusions

Task 2 of Project T10022 comprised the detailed concentration-response analysis of individual benzimidazoles in the CBMN assay and for **Task 4** additional, non-benzimidazole aneugens and clastogens were examined. Further, the cytotoxicity for all test compounds was assessed in the MTT assay.

- Seven out of eight benzimidazoles, four out of five clastogens as well as all tested non-benzimidazole aneugens induced MNs in the CBMN assay using CHO-K1 cells.

- All effective compounds produced monotonic and nonlinear concentration-response relationships in the CBMN assay with no detectable cytotoxicity at low effect concentrations.

- A minimum of three independent experiments per individual compound was considered as sufficient to accurately estimate their concentration-response relationships. Additional experiments were only required if the initial range finding experiment did not contain enough test concentrations within the effective range. Data from all 15 test compounds confirmed a high reproducibility of the CBMN assay.

- Statistical analysis of the concentration-response data of the benzimidazoles suggested the inclusion of a threshold parameter in the regression modelling. This model assumption was expanded to all compounds and mixtures and taken into account in predicting mixture effects according to CA and IA.

- Cytotoxicity assessment of all compounds in the MTT assay demonstrated that the data quality of the CBMN assay (data variation, reproducibility) was not affected by cytotoxicity as long as the cytotoxicity of test concentrations was below 40%. Therefore, only data from concentrations below the MTT-IC_{40} were included in the regression modelling and mixture effect predictions (**Tasks 3 and 4)**.

- All 15 compounds were considered as appropriate for inclusion in mixture studies

Chapter 4:
Mixture Experimentation – Mixtures of Benzimidazoles and Combinations of Benzimidazoles and Non-benzimidazole Genotoxins

Tasks 3 and 4

Summary

Tasks 3 and 4 of Project T10022 comprised the assessment of the mixture effects of benzimidazole mixtures and combinations of benzimidazole and non-benzimidazole genotoxins. In summary we found that:

- For three multi-component mixtures (mixtures I, II and III) we established experimental designs where CA and IA produced additivity predictions that differed sufficiently to be discriminated experimentally and statistically. This was not possible for a binary mixture of two aneugens (mixture IV).

- For all mixtures CA predicted higher mixture responses than IA, independent of the number of mixture components and the investigated effect levels.

- All mixtures produced clear monotonic and nonlinear concentration-response relationships in the CBMN assay, with no (or only weak) cytotoxicity at low effect concentrations.

- A greater overlap of the effective concentration ranges in CBMN assay with cytotoxicity was more likely to increase data variability at higher mixture concentrations.

- The mixture effects of seven benzimidazoles (mixture I) were accurately predicted by CA, and were consistently underestimated by IA. Mixture concentrations at which none of the included benzimidazoles had a statistically significant effect on their own produced highly significant responses.

- The combination effects of a benzimidazole with four non-benzimidazole aneugens (mixture II) were slightly overestimated by CA, but similarly underestimated by IA. Again, a highly statistically significant mixture effect was observed when all compounds were tested in combination of their individual threshold concentrations. Higher mixture concentrations showed increased data variability, probably due to higher mixture cytotoxicity. This was accompanied by a higher level of generally disrupted cell nuclei, pointing to a higher level of mitotic dysfunction.

- The combined effects of a benzimidazole and four non-benzimidazole clastogens (mixture III) were overestimated by CA. At lower mixture concentrations IA underestimated the effects, whereas at high concentrations the effects were within the IA prediction. Less cytotoxicity and nuclear disruption was observed, indicating that the deviation from additivity could be due to the differences in mechanisms of action of the mixture components.

- A binary mixture of a benzimidazole and a non-benzimidazole aneugen chosen by their differences in tubulin binding sites (mixture IV) allowed only a poor discrimination between CA and IA. However, it allowed to conclude that the mixture responses were in agreement with predictions from both additivity models. Here we also observed increased data variability at higher concentrations, probably due to higher cytotoxicity and a high level of more severe mitotic dysfunction at these concentrations.

Introduction

The following chapter presents the outcomes from all the mixture experiments carried out in this project (**Tasks 3 and 4**).

Using the concentration-response data produced for all individual MN inducing compounds, we designed sets of mixtures to be tested in the CBMN assay using CHO-K1 cells.

The first aim was to investigate the combined effects of a set of benzimidazoles (**Task 3**: "Assessment of mixture effects of combinations of benzimidazoles"). One important aspect of the project was to choose an experimental mixture design that provided a clear discrimination between the predictions from the two competing mixture models CA and IA. This would then allow an unambiguous decision about which of the two prediction models most accurately describes the observed mixture effects, in line with the aims of this project. To achieve this discrimination, we always selected the highest possible number of compounds for inclusion in the mixture, assuming that the quality of their concentration-response data was sufficiently high for mixture experimentation.

Firstly, seven of the eight tested benzimidazoles reproducibly induced MNs in a concentration dependent fashion in our assay system and were therefore included in the mixture testing.

Secondly, the next test mixture was a combination of aneugens, including benzimidazole and non-benzimidazole compounds (**Task 4**: "Assessment of mixture effects of combinations of benzimidazoles and non-benzimidazole aneugens").

Thirdly, we decided to compose a mixture not only including aneugenic benzimidazoles, but also sets of clastogens which exhibit a variety of mechanisms of action.

Finally, a binary mixture was tested composed of a benzimidazole and a non-benzimidazole aneugen to demonstrate the (im-) practicability of testing binary mixtures to discriminate between CA and IA.

In addition to the results from mixture effect predictions and experimental testing of the combination effects, the assessment of the mixtures' cytotoxicity in the MTT assay will be presented.

Results and discussion: Mixture experimentation

Combined effects of seven benzimidazoles (Mixture I)

During **Task 3** of the project the combined effects of the seven benzimidazoles which were positive in the CBMN assay were assessed (mixture I, (albendazole, albendazole oxide, benomyl, carbendazim, flubendazole, mebendazole and oxibendazole)). First, the data from the concentration-response analyses in **Task 2** (Table 4) was used to predict the mixture effects according to the two prediction models CA and IA. The mixture was designed by combining the benzimidazoles at concentrations proportional to their estimated threshold concentrations (Table 8). As shown in Figure 12A, the fixed-mixture ratio design resulted in two distinct prediction curves for the expected mixture effect for the two models, CA (red) and IA (blue), indicating that the experimental design was sufficient do allow a clear discrimination between the two prediction curves and observed mixture effects. The 95% confidence intervals (CI) for both predictions (dashed lines in the respective colour) further support the feasibility of discrimination between the two models. Due to minor experimental variations in the baseline levels of MN between the experiments, the estimated baseline rates differed slightly between the single compounds. To take this variation into account, we calculated two different IA prediction curves, based on the highest or lowest estimated baselines from the single compounds. As Figure 12A shows, there were only marginal differences between the two IA prediction curves. The CA prediction curve covers the entire range of potential baseline rates. The concentration-effect curves of the individual benzimidazoles at concentrations present within the mixture are also shown (light brown).

Assuming that the estimated threshold concentrations were close to the true "zero" effect concentrations, we expected that there should be no mixture effect under the IA assumption at and below the mixture concentrations equal to the sum of the individual compounds' combined threshold concentrations. CA on the other hand predicted a clear additive effect at and below this mixture concentration.

Next, the mixture was tested experimentally in the CBMN assay. Pooled data from three independent experiments are shown in Figure 12A (black dots). The experimental data clearly indicates that the concentration-response for MN induction by the combined benzimidazoles agreed well with the prediction curve for CA. The threshold concentration estimated from experimental data was almost one order of magnitude lower than the mixture threshold predicted by IA, but in good agreement with the CA prediction. The estimated model parameters for the mixture, as well as the baseline rate of MN induction and the mixture threshold concentration are presented in Table 5. A comparison of the statistical uncertainty of the two prediction models and the experimental data for 5% and 10% effects are provided in Table 7.

The cytotoxicity of mixture I was also assessed in the MTT assay (Figure 12B, Table 6) and the grey areas in Figure 12A indicate the concentration range where more than 40% cytotoxicity was observed. The cytotoxicity measured in the MTT agreed well with the combined toxicity assumed for the individual compounds. The experimentally determined MTT-IC_{40} of the mixture ($9.32E^{-6}$ M with a 95% CI of $6.46E^{-6}$ M to $1.35\ E^{-5}$ M) was in good agreement with CA which estimated an MTT-IC_{40} of $7.62E^{-6}$ M, whereas IA underestimated the combined cytotoxic effects ($5.0E^{-6}$ M). The IC_{40} of $9.32E^{-6}$ M for the mixture toxicity was also sufficiently above the concentration range tested for discrimination of CA and IA in the CBMN assay.

Figure 12:
Predicted and observed mixture effects of seven benzimidazoles in the CBMN assay and mixture cytotoxicity. A) The mixture of the seven CBMN positive benzimidazoles (albendazole, albendazole oxide, benomyl, carbendazim, flubendazole, mebendazole and oxibendazole) was designed at a fixed mixture ratio, using the threshold concentrations of the single compounds. The mixture effects were predicted according to CA (red curve) and IA (blue curve). The red and blue dashed lines indicate the 95% confidence intervals for the CA and IA predictions. The light brown curves show the effect of the individual compounds at the concentrations present in the mixture. Experimental concentration-response analysis of the mixture was conducted in the CBMN assay using CHO-K1 cells. The activity in the assay is shown as percentage of MN positive binucleated (bn) cells. Pooled data from three independent experiments are shown as black dots, the red horizontal line corresponds to the mean baseline MNs for the experimental data and the vertical dashed black line to the experimental threshold concentration estimated for the mixture.
B) Cytotoxicity of mixture I in the MTT assay. Black dots show the data from at least three independent experiments. The red curve shows the respective regression curve with its 95% confidence intervals (dashed red lines). The box and whisker plot shows the positive and negative controls at zero and one respectively.

A)

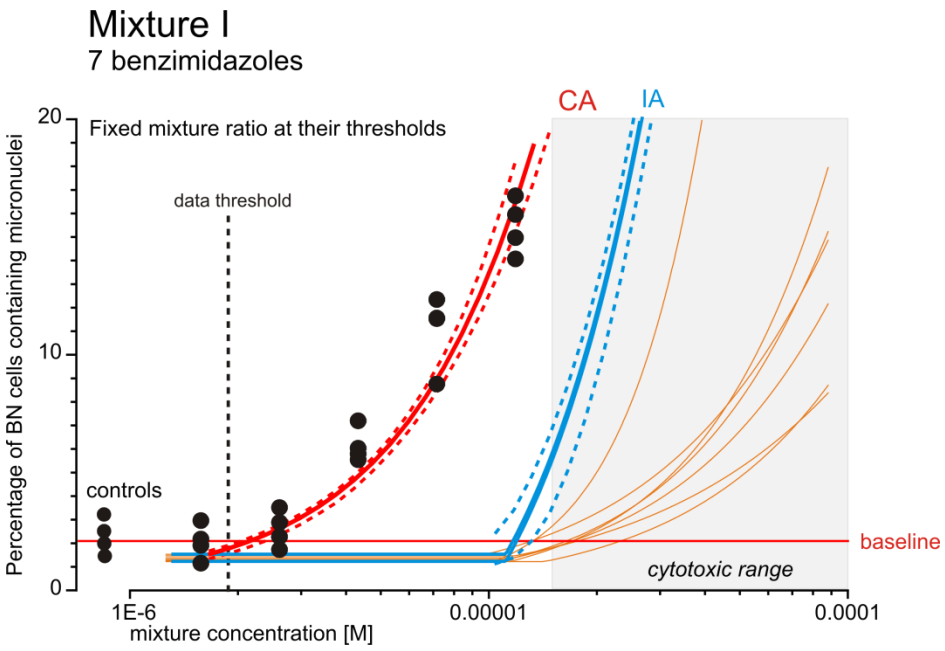

B)

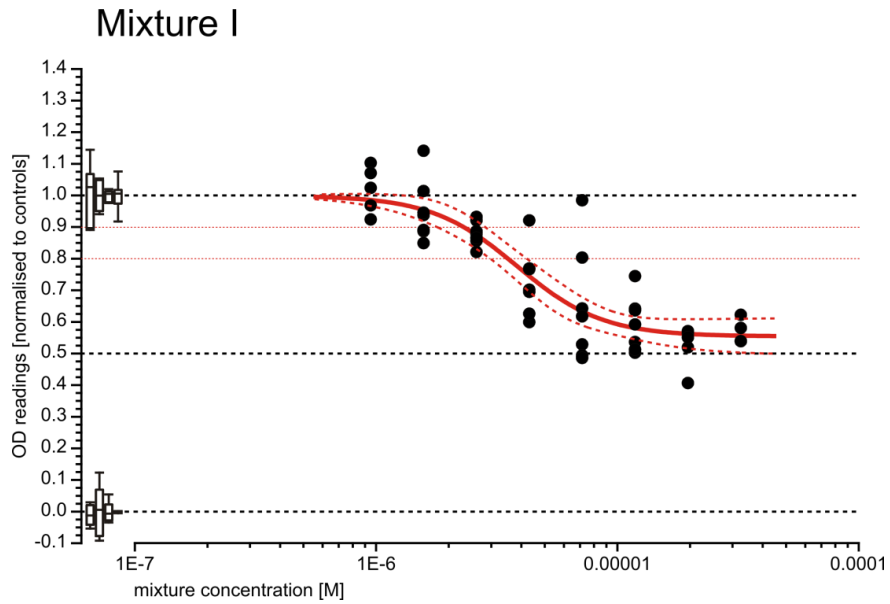

Combined effects of benzimidazole and non-benzimidazole genotoxins

The aim of **Task 4** was to combine benzimidazoles with non-benzimidazole aneugens to determine whether the effects of such mixtures would be predictable by CA, in the same way as a combination of benzimidazoles only. The agents in this mixture all interfere with tubulin, however have different binding sites and different mechanisms of action (i.e. blocking of microtubule polymerisation versus depolymerisation). We further decided to test a mixture of compounds with mixed, aneugenic and clastogenic, modes of action.

Combined effects of benzimidazole and non-benzimidazole aneugens (mixture II)

One benzimidazole (flubendazole) was combined with the four aneugens colchicine, griseofulvin, paclitaxel and vinblastine. Flubendazole was chosen due to its potency and data reproducibility. Colchicine, vinblastine and flubendazole are all assumed to share the same tubulin binding site and inhibit the polymerisation of microtubules. Griseofulvin binds to a different site but also blocks microtubule polymerisation. Paclitaxel occupies a different binding site and shows an entirely different mode of action: it causes inhibition of microtubule depolymerisation. The estimated threshold levels of the individual aneugens were used to design mixture II at a fixed mixture ratio (Table 8). The concentration-response data for the five aneugens (Table 4) was used to predict the mixture effects according to CA and IA. The two prediction models again produced two distinct prediction curves as shown in Figure 13A (CA (red) and IA (blue)). Compared to the predictions for mixture I, these prediction curves exhibited greater variations and correspondingly larger CIs (dashed lines in the respective colour), which was due to the lower number of compounds within the mixture and a higher data variation observed for some of the aneugens (probably as result of a higher overlap of aneugenic and cytotoxic concentration ranges). However, the two prediction curves were still clearly distinguishable. Again two curves were calculated for IA to take into account the variations in baseline levels of MN between the experiments. The concentration-effect curves of the individual aneugens at concentrations present within the mixture are also shown (light brown).

CA predicted a clear additive effect at the sum of the individual threshold concentrations, whereas for IA no effect was to be expected.

The experimental testing of mixture II in the CBMN assay (Figure 13A, black dots) resulted in a concentration-response that fell within the prediction window defined by the CA and IA curves. Correspondingly, CA slightly overestimated the observed effects, while IA underestimated the mixture effects. The estimated model parameters for the mixture, as well as the baseline rate of MN induction and the mixture threshold concentration are presented in Table 5. The statistical uncertainty of the two prediction models and the data for 5% and 10% effects are compared in Table 7. Although the data did not follow CA, there was still a significant effect observed at the sum of the individual thresholds, which was predicted as non-effective by IA. These observations were best described by a mixed model, where the combined effects of flubendazole, colchicine, griseofulvin and vinblastine were first predicted with CA, followed by an IA prediction of the effects of this group combined with paclitaxel (green curve in Figure 13B) .

The cytotoxicity of mixture II was assessed in the MTT assay (Figure 13C, Table 6) and the grey areas in Figure 13A indicate the concentration range where more than 40% cytotoxicity was observed. The measured MTT- IC_{20} ($3.53E^{-6}$ M) agreed with the combined toxicity predicted by CA ($2.01E^{-6}$ M) and was underestimated by IA ($9.2E^{-6}$ M). For this mixture, there was some overlap of cytotoxicity with the genotoxic concentration range.

Figure 13:
Predicted and observed mixture effects of Mixture II in the CBMN assay and mixture cytotoxicity.
A) The mixture of five CBMN positive aneugens (flubendazole, colchicine, griseofulvin, paclitaxel and vinblastine) was designed at a fixed mixture ratio, using the threshold concentrations of the single compounds. The mixture effects were predicted according to CA (red curve) and IA (blue curve). The red and blue dashed lines indicate the 95% confidence intervals for the CA and IA predictions. The light brown curves show the effect of the individual compounds at the concentrations present in the mixture. Experimental concentration-response analysis of the mixture was conducted in the CBMN assay using CHO-K1 cells. The activity in the assay is shown as percentage of MN positive binucleated (bn) cells. Pooled data from three independent experiments are shown as black dots, the red horizontal line corresponds to the mean baseline MNs for the experimental data and the vertical dashed black line to the experimental threshold concentration estimated for the mixture.
B) Prediction of the mixture effects of Mixture II by a combined CA&IA model (green curve). The combined effects of flubendazole, colchicine, griseofulvin and vinblastine were predicted by CA and the combination of this group with paclitaxel was predicted by IA.
C) Cytotoxicity of mixture II in the MTT assay. Black dots show the data from at least two independent experiments. The red curve shows the respective regression curve with its 95% confidence intervals (dashed red lines). The box and whisker plot shows the positive and negative controls at zero and one respectively.

A)

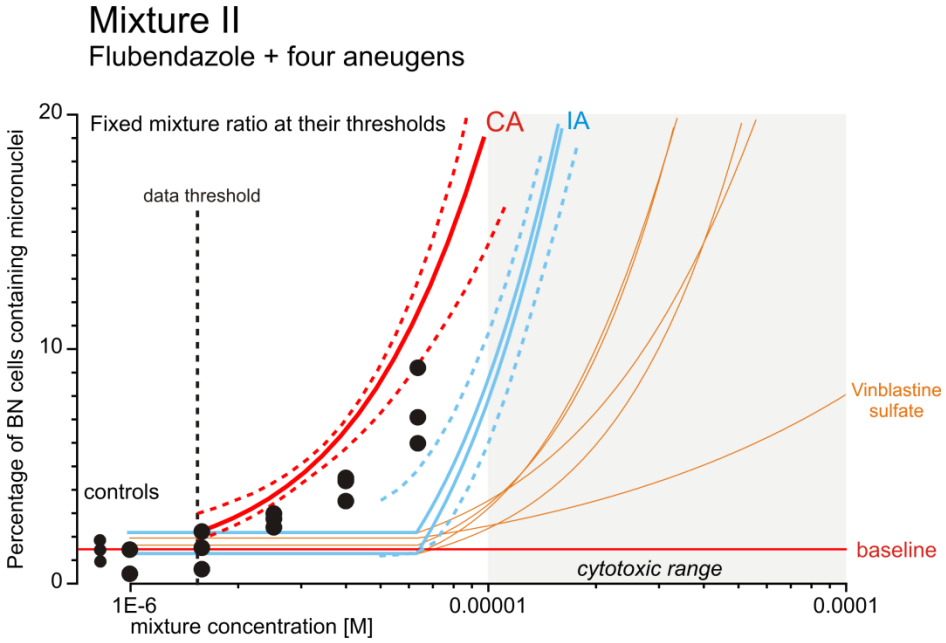

B)

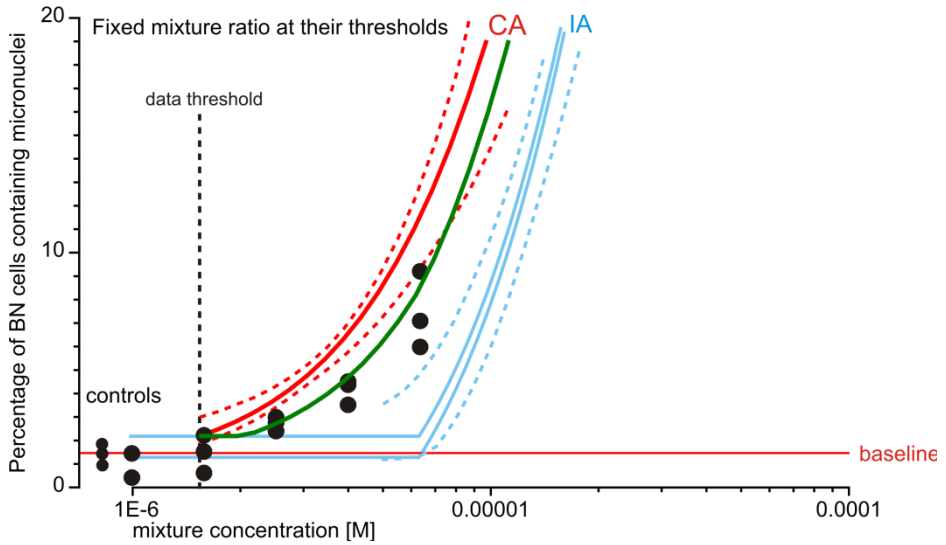

C)

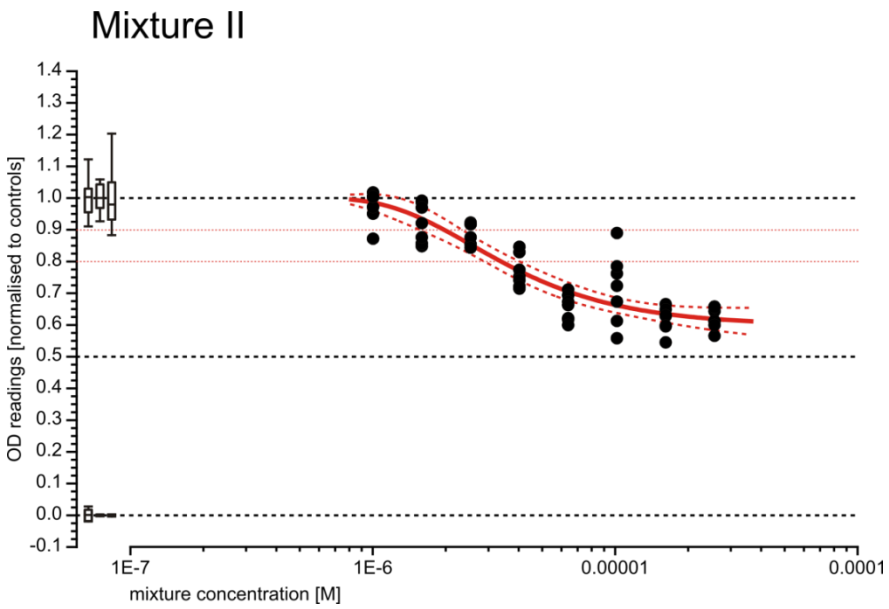
Mixture II
OD readings [normalised to controls]
1.4
1.3
1.2
1.1
1.0
0.9
0.8
0.7
0.6
0.5
0.4
0.3
0.2
0.1
0.0
-0.1
1E-7
1E-6
0.00001
0.0001
mixture concentration [M]

Combined effects of a benzimidazole and non-benzimidazole clastogens (mixture III)

A five component mixture of flubendazole and the four clastogens doxorubicin, etoposide, melphalan and mitomycin C (mixture IV) was tested to investigate the combined effects of genotoxins with mechanisms of action which we considered as very dissimilar for our assay endpoint. The aneugen flubendazole inhibits microtubule polymerisation, the clastogens melphalan and mitomycin C induce MN by DNA alkylation, albeit at different sites. Etoposide is an inhibitor of topoisomerase II and doxorubicin interacts with DNA by intercalation. Again, the estimated threshold levels of the individual compounds were used to design mixture III at a fixed mixture ratio (Table 8). The mixture effects according to CA and IA were predicted using the concentration-response data for flubendazole and the four clastogens (Table 4). The two prediction models produced two distinct prediction curves as shown in Figure 14A (CA (red) and IA (blue)) which were slightly closer to each other than in the previous mixtures. However, the CIs for the prediction curves (dashed lines in the respective colour), showed no overlap of the two curves over the sub-cytotoxic concentration range. As before, two curves are shown for IA to take account of the variations in baseline levels of MN between the experiments. The concentration-effect curves of the individual aneugens at concentrations present within the mixture are shown in light brown.

At the sum of the individual threshold concentrations, no effect was predicted by IA, but a clear additive effect was to be expected according to CA.

The responses of mixture III fell between the two prediction curves of CA and IA (Figure 14A, black dots). The estimated model parameters for the mixture, as well as the baseline rate of MN induction and the mixture threshold concentration are presented in Table 5. The statistical uncertainty of the two prediction models and the experimental data for 5% and 10% effects are compared in Table 7. CA slightly overestimated the mixture effect over the entire tested concentration range. At higher mixture concentrations, the mixture effects were better described by IA. However, at lower mixture concentrations, especially at the sum of the individual threshold concentrations, IA clearly underestimated the experimentally observed combination effects. Again, these findings could be described by a combined model of CA and IA. In a first step, we combined the two clastogens doxorubicin and etoposide in one group and the other two clastogens melphalan and mitomycin C in a second group and predicted their group effects by CA. Next, the combined effects of group one, group two and flubendazole were predicted by IA. Taking into account the variations in the baseline levels in MN for the different groups, this lead to two close prediction curves, similar to that seem in the IA prediction, which was in good agreement with the experimental data (green curves in Figure 14B).

Mixture III was also tested in the MTT assay (Figure 14C, Table 6). Its cytotoxicity agreed well with the combined toxicity assumed for the individual compounds. The measured MTT-IC_{40} ($1.08E^{-6}$ M) was in agreement with the mixture toxicity predicted by CA ($1.3E^{-6}$ M) and was underestimated by IA ($2.44E^{-5}$ M). The mixture's IC_{40} of $1.08E^{-6}$ M was well above the concentration range tested for discrimination of CA and IA in the CBMN assay.

Figure 14:
Predicted and observed mixture effects of Mixture III in the CBMN assay and mixture cytotoxicity.
A) The mixture of the one benzimidazole aneugen (flubendazole) with four clastogens (doxorubicin, etoposide, melphalan and mitomycin C) was designed at a fixed mixture ratio, using the threshold concentrations of the single compounds. The mixture effects were predicted according to CA (red curve) and IA (blue curve). The red and blue dashed lines indicate the 95% confidence intervals for the CA and IA predictions. The light brown curves show the effect of the individual compounds at the concentrations present in the mixture. Experimental concentration-response analysis of the mixture was conducted in the CBMN assay using CHO-K1 cells. The activity in the assay is shown as percentage of MN positive binucleated (bn) cells. Pooled data from three independent experiments are shown as black dots, the red horizontal line corresponds to the mean baseline MNs for the experimental data and the vertical dashed black line to the experimental threshold concentration estimated for the mixture.
B) Prediction of the mixture effects of Mixture II by a combined CA&IA model (green curves). The combined effects of doxorubicin and etoposide (group I) as well as melphalan and mitomycin C (group II) were predicted by CA, respectively and the combination of groups I, II and flubendazole was predicted by IA.
C) Cytotoxicity of mixture III in the MTT assay. Black dots show the data from at least two independent experiments. The red curve shows the respective regression curve with its 95% confidence intervals (dashed red lines). The box and whisker plot shows the positive and negative controls at zero and one respectively.

A)

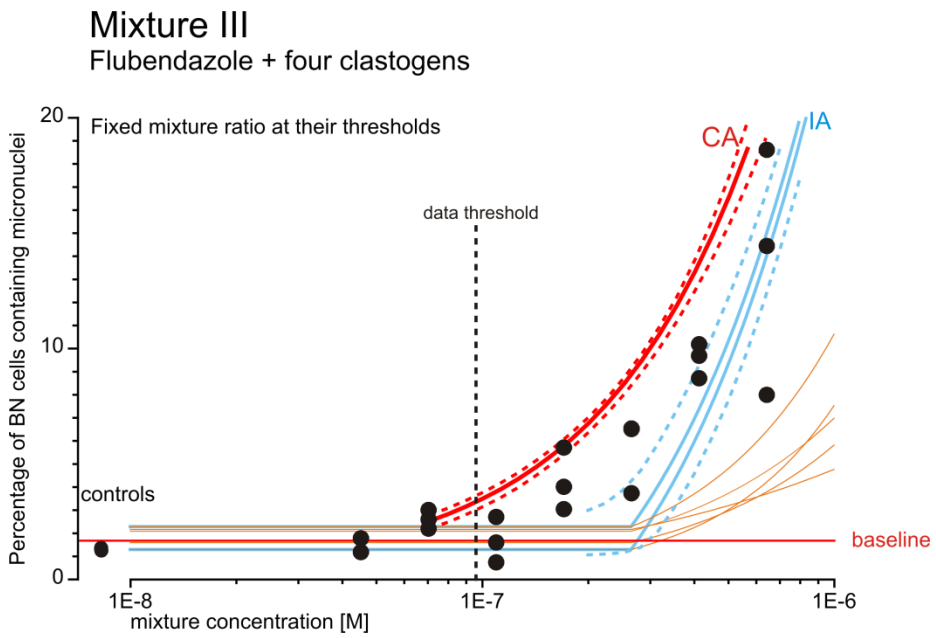

B)

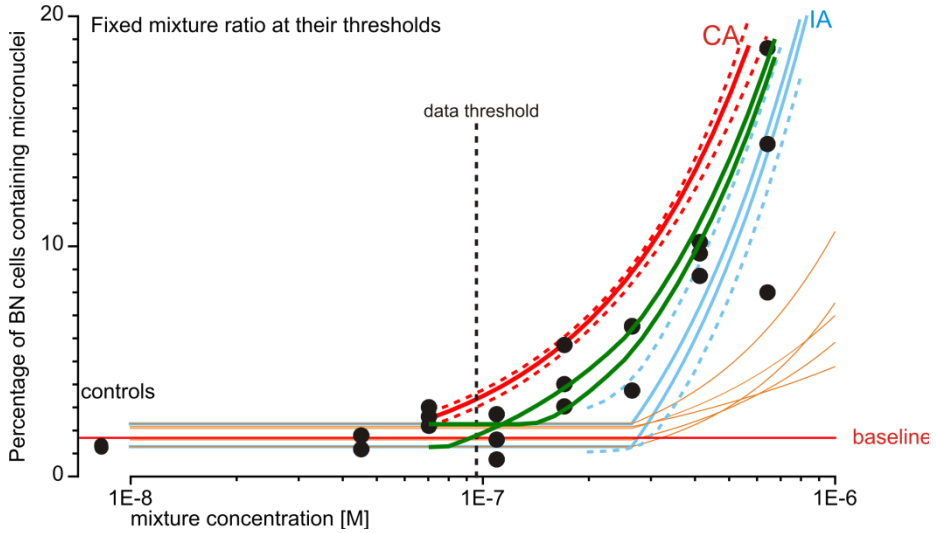

C)

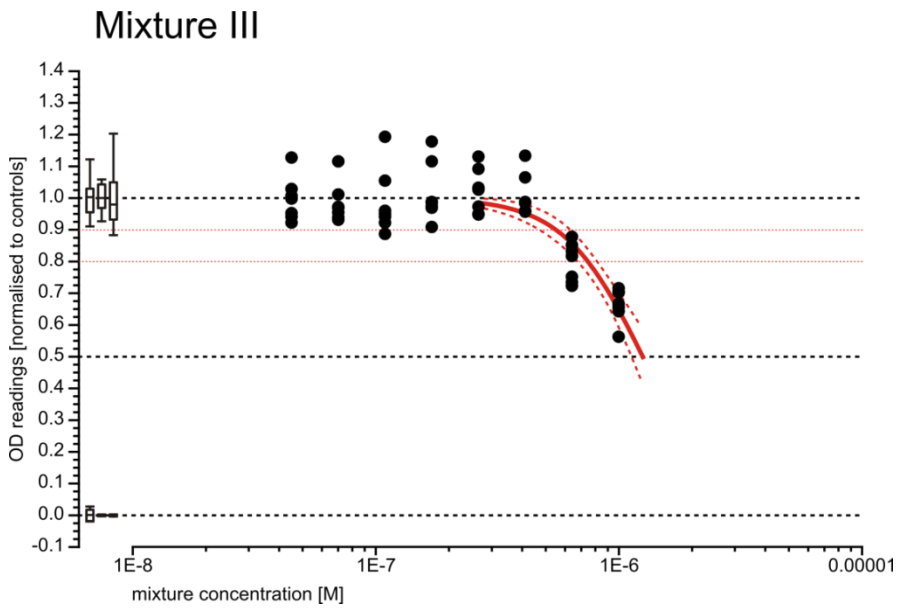
Mixture III
OD readings [normalised to controls]
1.4
1.3
1.2
1.1
1.0
0.9
0.8
0.7
0.6
0.5
0.4
0.3
0.2
0.1
0.0
-0.1
1E-8
1E-7
1E-6
0.00001
mixture concentration [M]

Combined effects of a benzimidazole and a non-benzimidazole aneugen (mixture IV)

Finally, a binary mixture of flubendazole and paclitaxel was tested (mixture IV). Although we considered binary mixtures in our test system as less useful for a sound comparative mixture assessment, we investigated its limitations by testing a mixture of two aneugens with distinct mechanisms of action at the microtubules (i.e. blocking of microtubule polymerisation by flubendazole versus depolymerisation by paclitaxel). Mixture IV was designed at a fixed mixture ratio using the estimated threshold levels of flubendazole and paclitaxel (Table 8) and their combined effects were predicted by CA and IA using their individual concentration-response data (Table 4). As expected, both mixture models produced prediction curves that were very close to each other over the entire tested concentration range (Figure 15A, CA (red) and IA (blue)). Moreover, their corresponding 95% confidence belts (dashed lines in the respective colour) overlapped, indicating that the statistical discrimination between the two predictions was rather poor. The reason for this poor discrimination are many fold: not only the low number of mixture components contributed to this dilemma, but also the differences in baseline levels of MN between the flubendazole and the paclitaxel data, and the high data variation of paclitaxel, probably caused by the largely overlapping aneugenic and cytotoxic concentration ranges. However, paclitaxel was the only aneugen tested that inhibits microtubule depolymerisation. The concentration-effect curves for the two individual aneugens at concentrations present within the mixture are shown in light brown.

For IA no effect was expected at the sum of the individual threshold concentrations and a small effect was predicted by CA.

The results from experimental testing of mixture IV are shown in Figure 15A (black dots) and the estimated model parameters for the mixture, as well as the baseline rate of MN induction and the mixture threshold concentration are presented in Table 5. The statistical uncertainty of the two prediction models and the experimental data for 5% and 10% effects are compared in Table 7.

The observed mixture effects were predicted equally well by both prediction models. The data showed a higher variability towards higher mixture concentrations, which was most likely due to a substantial overlap between aneugenic and cytotoxic concentration ranges (MTT data in Figure 15B, Table 6 and the grey areas in Figure 15A). The cytotoxic effects of this mixture (MTT-IC_{40} $3.68E^{-7}$ M) were predicted well by CA (MTT-IC_{40} $3.91E^{-7}$ M) whereas IA (MTT-IC_{40} $7.86E^{-7}$ M) underestimated the effects.

Figure 15:
Predicted and observed mixture effects of Mixture IV in the CBMN assay and mixture cytotoxicity.
A) The binary mixture of flubendazole and paclitaxel was designed at a fixed mixture ratio, using the threshold concentrations of the single compounds. The mixture effects were predicted according to CA (red curve) and IA (blue curve). The red and blue dashed lines indicate the 95% confidence intervals for the CA and IA predictions. The light brown curves show the effect of the individual compounds at the concentrations present in the mixture. Experimental concentration-response analysis of the mixture was conducted in the CBMN assay using CHO-K1 cells. The activity in the assay is shown as percentage of MN positive binucleated (bn) cells. Pooled data from three independent experiments are shown as black dots, the red horizontal line corresponds to the mean baseline MNs for the experimental data and the vertical dashed black line to the experimental threshold concentration estimated for the mixture.
B) Cytotoxicity of mixture IV in the MTT assay. Black dots show the data from at least two independent experiments. The red curve shows the respective regression curve with its 95% confidence intervals (dashed red lines). The box and whisker plot shows the positive and negative controls at zero and one respectively.

A)

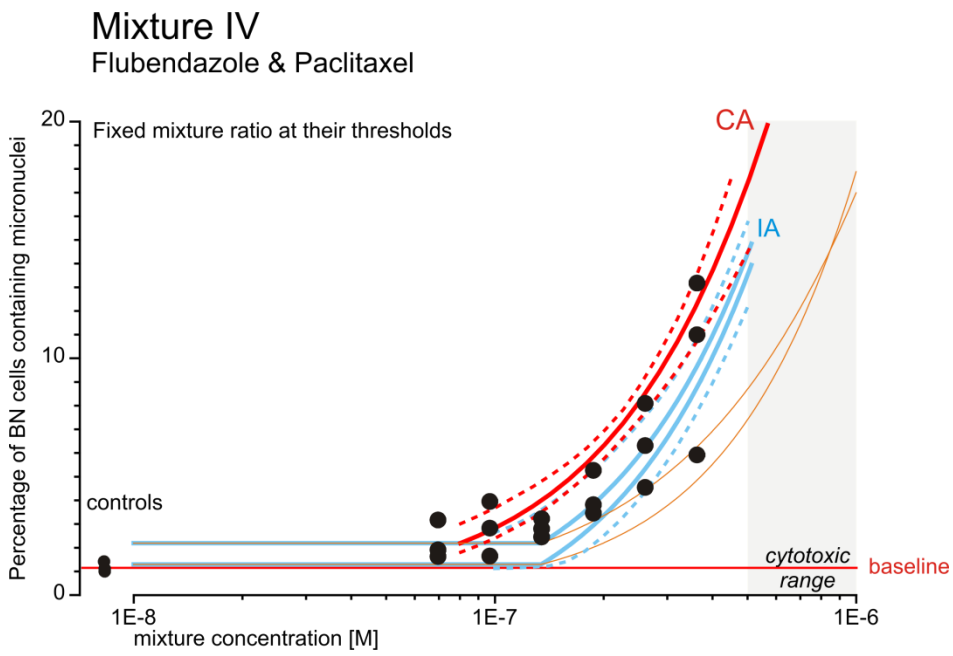

B)

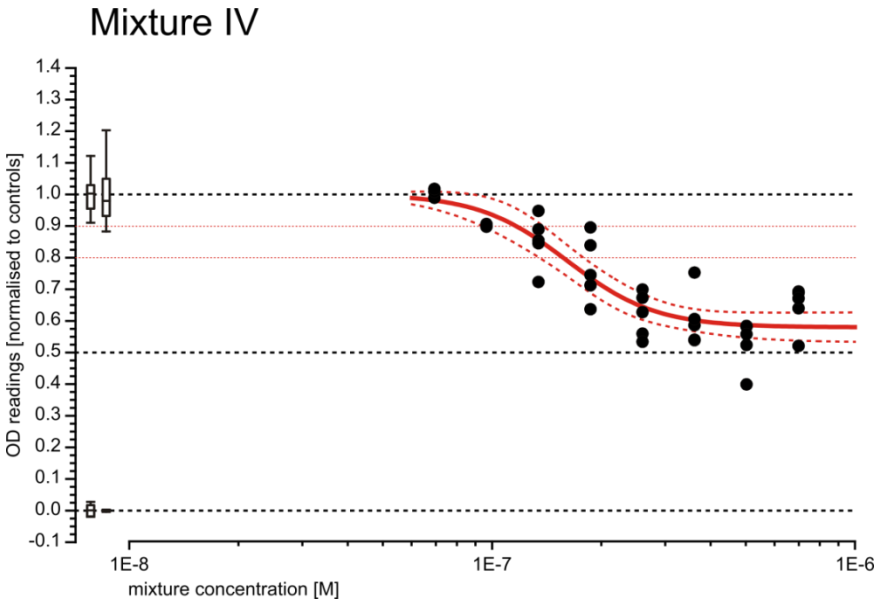

Table 5: Threshold concentration-response models for the mixtures in the CBMN assay.

Substance	model	model parameter $\hat{\theta}_1$	$\hat{\theta}_2$	$\hat{d}$	baseline rate* (95% CI)		threshold concentration (95%CI) [M]	
Mixtures								
Mix I (benzimidazoles)	weibull	-3.861	2.813	-5.726	2.08%	(1.92% -2.25%)	1.88E-06	(1.66E-06 -2.13E-06)
Mix II (aneugens)	weibull	-4.299	2.561	-5.857	1.34%	(1.10%-1.60%)	1.39E-06	(1.05E-06-1.83E-06)
Mix III (clastogens)	weibull	-4.088	2.855	-7.018	1.66%	(1.45%-1.87%)	9.59E-08	(8.28E-08-1.11E-07)
Mix IV (paclitaxel & flubendazole	weibull	4.479	2.036	-7.418	1.13%	(0.87%-1.39%)	3.82E-08	(2.64E-08-5.52E-08)

* baseline rate is expressed as percentage; $\hat{\theta}_1, \hat{\theta}_2$ and $\hat{d}$ are estimates of the unknown model parameter θ_1, θ_2 and d.

Table 6: Cytotoxicity of the mixtures in the MTT assay

Substance	Concentration-Response Function RM	$\hat{\theta}_1$	$\hat{\theta}_2$	$\hat{\theta}_3$	$\hat{\theta}_{min}$	θ_{max}	IC_{10} M [CI]		IC_{20} M [CI]		IC_{40} M [CI]	
Mixtures												
Mixture I	logit	-30.58	-5.65	--	0.55	1	2.31E-6	[1.83E-6 - 2.92E-6]	3.53E-6	[2.99E-06 - 4.17E-6]	9.32E-6	[6.46E-6 - 1.35E-5]
Mixture II	weibull	-16.35	-2.92	--	0.59	1	1.95E-6	[1.60E-6 - 2.38E-6]	3.35E-6	[2.85E-6 - 3.95E-6]	1.19E-4	n.d.
Mixture III	logit	-36.13	-6.12	--	0*	1	5.49E-7	[4.72E-7 - 6.38E-7]	7.45E-7	[6.80E-7 - 8.16E-7]	1.08E-6	[9.74E-7 - 1.19E-6]
Mixture IV	logit	-55.66	-8.19	--	0.58	1	1.16E-7	[9.46E-8 - 1.43E-7]	1.57E-7	[1.37E-7 - 1.79E-7]	3.68E-7	[2.25E-7 - 6.02E-7]

IC_{10}, IC_{20}, IC_{40}: concentrations provoking 10%, 20% and 40% lower OD readings to the negative controls, respectively. Values in brackets denote the upper and lower limits of the approximate 95% confidence interval; the column "RM" indicates the mathematical regression function as defined at Scholze *et al.* (2001): $\hat{\theta}_1, \hat{\theta}_2, \hat{\theta}_3, \hat{\theta}_{min}$ estimated model parameters, given for concentrations expressed in M (rounded values), θ_{max} were not estimated, but set to 1 relating to the mean value of the negative controls; * hold fixed; ">" indicates highest test concentration;

Table 7: Statistical uncertainty of predicted and observed effect concentrations for mixtures

Induction of MN	Effect concentration ECx_{mix} [M]					
	Observed		Predicted by CA		Predicted by IA	
	Mean	95% CI	Mean	95% CI	Mean*	95% CI
Mixture 1: seven benzimidazoles (ratio as defined in Table 8*)*						
5 %	3.94E-6	[3.68E-6 - 4.22E-6]	4.46E-6	[4.31E-6 - 4.73E-6]	1.36E-5 - 1.39E-5	[1.27E-5 - 1.58E-5]
10 %	7.35E-6	[6.90E-6 - 7.84E-6]	7.86E-6	[7.47E-6 - 8.31E-6]	1.77E-5 - 1.79E-5	[1.68E-5 - 1.98E-5]
Mixture 2: five aneugens (ratio as defined in Table 8*)*						
5 %	4.59E-6	[4.17E-6 - 5.06E-6]	3.24E-6	[3.00E-6 - 3.54E-6]	8.07E-6 - 8.53E-6	[6.50E-6 - 9.36E-6]
10 %	8.77E-6	[7.27E-6 - 1.06E-5]	5.72E-6	[5.31E-6 - 6.88E-6]	1.08E-5 - 1.13E-5	[9.70E-6 - 1.24E-5]
Mixture 3: Flubendazole & four clastogens (ratio as defined in Table 8*)*						
5 %	2.36E-7	[2.22E-7 - 2.51E-7]	1.47E-7	[1.36E-7 - 1.56E-7]	3.44E-7 - 3.74E-7	[2.88E-7 - 4.15E-7]
10 %	4.22E-7	[4.06E-7 - 4.38E-7]	3.01E-7	[2.90E-7 - 3.15E-7]	4.92E-7 - 5.23E-7	[4.37E-7 - 5.68E-7]
Mixture 4: Flubendazole & paclitaxel (ratio as defined in Table 8*)*						
5 %	2.10E-7	[1.93E-7 - 2.30E-7]	1.64E-7	[1.41E-7 - 1.79E-7]	2.23E-7 - 2.52E-7	[1.80E-7 - 2.84E-7]
10 %	4.75E-7	[3.99E-7 - 5.64E-7]	3.02E-7	[2.81E-7 - 3.39E-7]	3.73E-7 - 3.98E-7	[3.39E-7 - 4.33E-7]

CA – Concentration Addition, IA – Independent Action, CI – Confidence Interval;

* predictions are calculated assuming lowest or highest observed baseline;

Conclusions

Task 3 of Project T10022 comprised the assessment of the mixture effects of combinations of benzimidazoles and for **Task 4** mixtures including benzimidazole and non-benzimidazole genotoxins were assessed.

- For all three tested multi-component mixtures (mixtures I, II and III) we established experimental designs where both models CA and IA produced additivity predictions that differed sufficiently to be discriminated experimentally and statistically. This was not possible for the mixture of two aneugens (mixture IV), thus the comparative assessment of this binary mixture was hampered.

- In all mixture experiments CA predicted higher mixture responses than IA, independent of the number of mixture components and the investigated effect levels.

- All mixtures produced clear monotonic and nonlinear concentration-response relationships in the CBMN assay, with no (or only weak) cytotoxicity at low effect concentrations.

- Generally, the more the effective concentration ranges in CBMN assay were overlapping with cytotoxicity, the more likely increased data variability at higher mixture concentrations was observed. Although we observed this phenomenon also for some of the individual aneugens, it was especially evident for mixtures II and IV, which both exhibited relatively shallow concentration-response curves in the MTT assay.

- The mixture of seven benzimidazoles (mixture I) exhibited combination effects that agreed well with the predictions by CA, whereas IA consistently underestimated the observed mixture responses. Mixture concentrations at which none of the included benzimidazoles were expected to produce an effect above the baseline on their own (i.e. equal or below their estimated threshold concentrations) produced highly significant responses in the CBMN assay. These were accurately predicted by CA.

- The combination of a benzimidazole with four non-benzimidazole aneugens (mixture II) produced responses that were slightly overestimated by CA, but similarly underestimated by IA. Again, a highly statistically significant mixture effect was observed when all compounds were tested in combination of their individual threshold concentrations. At higher mixture concentrations, we observed increased data variability, probably due to higher mixture cytotoxicity. Here, we also observed a higher level of generally disrupted cell nuclei was observed, which could not be taken into account by the automated micronucleus scoring. Thus, lower MN counts at higher concentrations were probably not due to a lower mixture aneugenicity, but to a higher level in mitotic dysfunction. On the other hand, taking into account the slightly different mechanisms of aneugenicity exhibited by paclitaxel as compared to the other aneugens, a combined model of CA and IA was able to produce a prediction curve that agreed well with the observed data.

- The combined effects of a benzimidazole and four non-benzimidazole clastogens (mixture III) were overestimated by CA and underestimated by IA. At lower

concentrations (e.g. at the sum of the individual threshold concentrations) IA predicted no detectable combination effects, which was in clear contrast to the observed responses, which were statistically significant above the baseline. In contrast, effects at high mixture concentrations were described well by IA. Low cytotoxicity had less impact on data variability and less overall nuclear disruption was observed at higher mixture concentrations. Therefore, the deviation from additivity could be due to the differences in mechanisms of action of the mixture components. This was supported by the finding that employing a mixed CA and IA model again predicted the observed mixture effects well.

- As flubendazole and paclitaxel disrupt the microtubules in different ways, we also tested their combination (mixture IV). Although the poor discrimination between both predictions prohibited *a priori* a clear assignment to one of the mixture models, the mixture experiment nevertheless showed that the mixture responses were in agreement with predictions from both additivity models. Especially, at high mixture concentrations the assessment was difficult due to the high data variability: again, we speculate that a relatively high cytotoxicity at these concentrations was responsible for the increased data variation. Furthermore, we observed a high level of generally disrupted nuclei, pointing to more severe mitotic dysfunction at these concentrations.

Chapter 5:
Discussion and Conclusions

Discussion and implications for cumulative risk assessment

Predictability of mixture effects of benzimidazoles

The main aim of this project was to assess whether the joint effects of benzimidazoles that can induce MN by disrupting microtubule formation can be predicted accurately by using the mixture assessment concept of CA. This was in response to a request from the UK COM. If it could be shown that these pesticides act together according to CA, disruption of microtubule polymerisation could be used as a criterion for grouping these chemicals for the purposes of cumulative risk assessment.

To achieve this aim, it was necessary to design a decisive experiment where, for a given combination of chemicals, the concepts of CA and IA yielded predictions that were sufficiently different from each other to be discriminated experimentally.

It is often the case that CA and IA produce identical mixture effect predictions, especially when the mixture to be assessed contains relatively small numbers of components. Prediction differences are driven by the number of mixture components, the slope of the concentration-response curves of the individual mixture components, the mixture ratio and the effect level chosen for analysis. With a given selection of chemicals, only mixture ratio and number of mixture components are accessible to experimental manipulation.

To be able to test a sufficiently high number of benzimidazoles, we first successfully implemented and validated an assay protocol followed by automated MN scoring system using image analysis. This allowed us to efficiently produce highly reproducible concentration response data of enough different benzimidazoles to be able to make significantly different predictions for CA and IA.

To ensure that all chemicals in the mixture contributed equally to the formation of MN, mixture ratios broadly proportional to the components' potency had to be chosen. This was realised by preparing serial dilutions of mixtures where the individual components were present according to their threshold concentrations for MN induction.

This left only the number of mixture components that could be varied to achieve a good discrimination between the predictions produced by CA and IA. These differences had to be sufficiently large to be discriminated considering the experimental variation of the MN assay.

We found that CA and IA mixture effect predictions that differed from each other sufficiently to be distinguishable decisively could be derived for combinations of the seven benzimidazoles albendazole, albendazole oxide, benomyl, carbendazim, flubendazole, mebendazole, oxibendazole. The experimentally observed MN frequencies agreed excellently with the CA prediction. The IA prediction fell short of the observed MN frequencies. Were IA applicable as the valid prediction and assessment concept, we expected that joint effects should not be observable when all components were combined at (or below) their threshold concentrations. This was not the case. Instead, there were clear combination effects at mixture concentrations where the individual components were present at levels well below their thresholds for MN induction, as was to be expected according to the CA principle.

A threshold concentration was defined as parameter in a mathematical concentration-response function and estimated by regression modelling. It presents the statistically most likely "zero" effect concentration at given data and model assumptions. Although it is unknown how accurately the "true" toxicological threshold was estimated by this statistical approach, we rule out that effects were wrongly estimated as "zero" baseline, which otherwise would have led to IA predictions that explained the combination effects for this mixture at low concentrations.

Due to the interactions of all mixture components with the same molecular site (tubulin subunits), one benzimidazole can be replaced with an equi-effective fraction of another to yield the same combination effect, as expected on the basis of CA.

These observations provide a strong incentive for subjecting combinations of benzimidazoles that disrupt microtubule polymerisation by interacting with the same site, the colchicine binding site, to cumulative risk assessment. Furthermore, our data show that CA is a valid concept for the accurate prediction of the resulting combination effects.

Combinations of flubendazole with other non-benzimidazole aneugens

Considering these experimental results, it appeared conceivable that combined effects on MN frequencies should also be expected with mixtures of agents that disrupt microtubule formation in different ways, e.g. by interacting with differing binding sites. Whether the resulting joint effects also follow the CA principle was a second question of interest.

Correspondingly, we relaxed the strict similarity criterion that was requested by COM and investigated a combination of the aneugenic benzimidazole flubendazole with other aneugens, such as colchicine, griseofulvin, paclitaxel and vinblastine. Benzimidazoles, colchicine and vinblastine all share a common tubulin binding site and block the polymerisation of microtubules. This is also believed to be the case for griseofulvin, which however binds to slightly different sites. Paclitaxel has a different tubulin binding site and inhibits microtubule depolymerisation. Although they slightly differ in their actions on the microtubules, all chemicals included in this mixture induced MN by disruption of the mitotic spindle apparatus.

This mixture induced MN frequencies that fell slightly short of the effects expected on the basis of CA, but were stronger than those predicted by IA. At the point where the stochastic principles of IA predicted background level effects, MN frequencies of between 5 and 10% were observed. Considering that this mixture was composed of three chemicals with identical tubulin binding sites, one agent with a different binding site and another that acts by stabilising tubulin polymerisation, the overall effect of the combination was best represented by a combination of CA and IA.

Although perfect agreement with CA was not achieved, this prediction concept provided responses that were quite close to the experimentally observed effects. CA can therefore be used to yield reasonable approximations of combinations of mixtures that incorporate agents beyond the chemical space represented by benzimidazoles.

Combinations of flubendazole with clastogens

Finally, we combined various agents capable of inducing MN by a variety of molecular mechanisms. This did not only include aneugens, but also clastogens. The benzimidazole flubendazole was combined with mitomycin C, etoposide, melphalan and doxorubicin.

Considering the modes of action involved in MN induction (it ranges from disrupting microtubule polymerisation to DNA intercalation with strand breakage and adduct formation), this is perhaps the mixture where the principles of IA were most likely to be applicable.

At the two highest concentrations, the effects of this mixture agreed with the IA prediction. However, at lower concentrations, where according to IA significant effects were not expected to occur, the MN frequencies were significantly higher than background levels. Thus, although this mixture came closest to the effects anticipated by IA, the IA principle was not fully realised.

At present we are unable to offer a mechanistic explanation for this observation. Similar to the mixture of various aneugens, the effects reflected a hybrid model of CA and IA. Future experimentation will have to investigate this by altering the composition of the mixture and including further agents with different modes of action for MN induction.

Implications for grouping criteria

Our results support the application of a mechanistic criterion – disruption of microtubule formation by binding to tubulin subunits – for the grouping of aneugenic benzimidazoles in the context of cumulative risk assessment. It would appear that this criterion can also be applied not only to benzimidazoles, but to any chemical capable of inducing MN by inhibition of microtubule polymerisation upon binding to tubulin at the same site as benzimidazoles.

Our results with the mixture composed of aneugens that induce MN by disrupting microtubule polymerisation in different ways (by binding to different sites on tubulin subunits and by blocking the degradation of microtubules) show that the grouping criterion can be extended to a wider range of aneugens. The overall criterion could be twofold: Ability to induce MN, and capability of interfering with microtubule polymerisation and depolymerisation. Although the agreement between observed and predicted mixture effects was not perfect in this case, CA provided reasonable approximations of the observed effects.

Finally, the effects observed with the mixture composed of aneugens and clastogens suggest that any chemical capable of inducing MN will act together with other agents that possess the same quality, to produce a joint effect that can be approximated by IA. It appears that cumulative risk assessment cannot be restricted to aneugens with more or less similar modes of action, but will have to encompass a wider range of chemicals, irrespective of precise molecular mechanisms. Here, the ability of inducing MN generally would be the appropriate grouping criterion, perhaps with IA as the relevant prediction model.

Our results show that the effects of the aneugen/clastogen mixture fall short of CA and come quite close to IA. This argues for the use of IA as a method not only for the evaluation of experimental results, but for cumulative risk assessment. However, cumulative risk assessment

methods based on IA do not exist (Kortenkamp et al. 2012), apart from the conjecture that no effect is expected when all components are present at or below their threshold levels. Crucially however, our work does not provide experimental evidence for this notion. There were statistically significant combination effects at and below the individual thresholds of all mixture components.

In the interest of conservatism, it therefore deserves serious consideration whether the ability of aneugens to induce MN can be used as a general grouping criterion, irrespective of mechanisms, for the purposes of cumulative risk assessment. However, many clastogens are also carcinogenic, and for these agents it is carcinogenicity, but not MN induction that is the critical effect which forms the basis for risk assessment. Because many aneugens that produce MN are not carcinogenic, the opportunity to group aneugens and clastogens has not arisen in the past. However, cumulative risk assessment that employs common effects as grouping criteria, will also have to rely on endpoints that do not form the basis of human health quality standards, such as acceptable daily intakes. Judged from this perspective, our observation of combined effects of aneugens and clastogens for MN induction will be of relevance for regulatory practice.

Chapter 6: Methodology

Chemicals and reagents

Albendazole (methyl [6-(propylthio)-1H-benzoimidazol-2-yl]carbamate, CAS# 54965-21-8), benomyl (methyl [1-[(butylamino)carbonyl]-1H-benzimidazol-2-yl]carbamate, CAS# 17804-35-2) carbendazim (methyl 1H-benzimidazol-2-yl carbamate, CAS# 10605-21-7), flubendazole (methyl N-[6-(4-fluorobenzoyl)-1H-benzimidazol-2-yl]carbamate, CAS# 31430-15-6), mebendazole (methyl (5-benzoyl-1H-benzimidazol-2-yl)carbamate, CAS# 31431-39-7), oxibendazole (methyl N-(6-propoxy-1H-benzimidazol-2-yl)carbamate, CAS# 20559-55-1), thiabendazole (4-(1H-1,3-benzodiazol-2-yl)-1,3-thiazole, CAS# 148-79-8), albendazole oxide (methyl [5-(propane-1-sulfinyl)-1H-benzoimidazol-2-yl]-carbamate, CAS# 54029-12-8), griseofulvin (2S)-trans-7-Chloro-2′,4,6-trimethoxy-6′-methylspiro(benzofuran-2[3H],1′-[2]cyclohexene)-3,4′-dione, CAS# 126-07-8), vinblastine sulfate (CAS# 143-67-9) paclitaxel (CAS# 33069-62-4), etoposide (4′-Demethylepipodophyllotoxin 9-(4,6-O-ethylidene-β-D-glucopyranoside), CAS# 33419-42-0), doxorubicin hydrochloride (CAS# 25316-40-9), melphalan (4-[bis(2-chloroethyl)amino]-L-phenylalanine, CAS# 148-82-3) and benzo(α)pyrene (CAS# 50-32-8) were purchased from Sigma at the highest purity available. MTT (3-(4,5-Dimethylthiazol-2-yl)-2,5-diphenyltetrazolium bromide), acridine orange (AO) and cytochalasin B (10 mg/ml) were also obtained from Sigma and Colchicine (CAS# 64-86-8) from Fluka. Mitomycin C was provided by Calbiochem, paraformaldehyde (PFA) by Avocado chemicals and dimethyl sulphoxide (DMSO, cell culture grade) by VWR and Triton X-100 by BDH. F12-K cell culture medium and HBSS buffer were purchased from Invitrogen.

General cell culture

CHO-K1 cells were purchased from the American Type Culture Collection (ATCC). They were routinely grown in 75 cm^2 canted neck tissue culture flasks in F-12K supplemented with 10% fetal calf serum (FCS) in a humidified incubator at 37°C with 5% CO_2. Cells were subcultured when confluent over a maximum of 10 passages and were tested regularly for *Mycoplasma* infections.

CBMN assay

The cytokinesis blocked micronuclei (CBMN) assay was initially performed in 25 cm^2 canted neck tissue culture flasks (T25). For concentration-response analysis it was miniaturised to 24 well plates. CHO-K1 cells were seeded in F12-K medium (10% FCS) at a density of 5 x 10^5 cells per T25 flask or 1.2 x 10^4 cells/well in 24 well plates and allowed to attach for 24 h. After this period, the medium was changed to F12-K medium containing the test compounds or mixtures. Chemicals were dissolved in DMSO and diluted in assay medium, the DMSO concentration never exceeding 0.5%. All MN inducing compounds and mixtures were tested in at least three independent experiments. For each experiment, a dilution series of eight concentrations of each compound or mixture was tested. The dilution factors were adjusted according to previous results to best test the whole active range of each compound. Controls were treated with solvent (DMSO, 0.5%) only (negative control), as reference compound for induction of micronuclei

served mitomycin C and/or flubendazole (positive control). Cells were incubated with test compounds for 24 h, then washed once with F12-K medium, before F12-K medium (10% FCS) supplemented with 3 µg/ml Cytochalasin B was added and incubated for a further 18 – 20 h. After this period the medium was changed to F12-K medium (10% FCS) and the cells left to recover for 1 - 2 h. The cells were harvested by trypsinisation, counted and centrifuged onto glass slides using a cyto-centrifuge for 10 min at 1,200 rpm. The final cell density on the slide was 5,000 to 10,000 cells. The cells were immediately fixed in 4% PFA (in PBS) for 10 min at room temperature. The fixed slides were washed for 2 x 5 min in PBS on a shaker, before staining them with 10 µg/ml acridine orange (in ddH_2O) for 10 min at room temperature. The slides were washed for 2 x 5 min in ddH_2O on a shaker, then dipped into ddH_2O, allowed to air-dry and mounted with Vectashield HardSet mounting medium containing DAPI (1.5 µg/ml, Vector Laboratories).

Automated image acquisition and micronucleus scoring

For automated image acquisition and MN scoring, a Pathfinder™ Cellscan µN platform for automated micronucleus assay scoring (IMSTAR) was used. It was equipped with an Olympus BX41 fluorescence microscope with an automated stage and employed the IMSTAR Pathfinder™ software for image acquisition and analysis. It could process up to four slides in one imaging step. Image analysis was started after acquisition of the first image.

MTT assay for cytotoxicity detection

A modified version of the 3-(4,5-dimethylthiazol-2-yl)-2,5-diphenyltetrazolium bromide (MTT) assay was carried out as described by Mosmann (1983). CHO-K1 cells were seeded at a density of 5000 cells/well in F12-K medium (10% FCS) in clear plastic 96 well plates. Cells were allowed to attach for 24 h before being treated with the test compounds. Chemicals were dissolved in DMSO and diluted in assay medium, the DMSO concentration never exceeding 0.5%. Samples were tested in duplicate. Controls were treated with solvent (DMSO) only (negative control) or with 1% Triton X-100 (positive control). After treatment for 24 h, the cells were washed once with F12-K medium, before F12-K medium (10% FCS) containing 3 µg/ml Cytochalasin B was added and the cells were incubated for a further 18 – 20 h. After this period the medium was changed to F12-K medium (10% FCS) and the cells left to recover for 1 – 2 h before the medium was removed and replaced with F12-K medium (10% FCS) containing 250 µg/ml MTT. Cells were incubated for 1 h with the MTT solution, allowing viable cells to reduce the yellow MTT to dark blue crystals of formazan. Next, the cells were washed once with HBSS buffer before adding DMSO to dissolve the formed formazan crystals for 30 min on a shaker. The optical density of solubilised formazan product was photometrically quantitated by reading the absorbance at 570 nm and 620 nm using a plate reader. The 570 nm readings were corrected for background by subtracting the 620 nm readings. Data was normalised by subtracting the average values of positive (Triton X-100) controls from sample values and the average of negative (solvent) control and then by dividing the so corrected sample values by the negative controls.

Biostatistical analysis of the CBMN assay

The induction of MNs in the CBMN assay is measured as the number of binucleated (bn) cells with at least one micronucleus ($N_{MN\geq1}$) in relation to all binucleated cells (N_{total}), and expressed as ratio r:

$$r=\frac{N_{MN\geq1}}{N_{total}}. \quad (1)$$

If all cells with at least one micronucleus count as "success", this "success" is a binary outcome. Because the number of successes from a definite sample size N_{total} is of interest, the success rate is estimated statistically by the binomial distribution. Consequently, treatment effects were analysed by quantal concentration-response analysis assuming binomially distributed data, and expressed as success probability p, e.g. a value of p=0.1 means that 10% of all binucleated cells are most likely to have at least one micronucleus. It should be noted that equal p estimates from different samples only give estimates of success probability of comparable reliability if the samples contain similar numbers of binucleated cells: an estimate p=0.1 on the basis of 100 binucleated cells is statistically less precise than one on the basis of 10,000 cells. Statistical analysis takes these imbalances into account.

As is typical for this assay, a low rate of micronuclei is always observed, even when the cells have not been exposed. This low response in “control cultures” is called baseline or spontaneous response. A common assumption is that this baseline rate is independent of treatment effects, i.e. a baseline rate higher than normal does not necessarily imply that all treatment-related MN rates are increased in the same (proportional) way. Baseline rates might vary from experiment to experiment (“inter-experimental variability”), and concentration-response analysis for individual compounds as well as quantitative mixture analysis must take this into account.

A further complication for the concentration-response analysis is that for the selected test chemicals and assay endpoint the dose threshold concept is assumed, i.e. the existence of a threshold concentration, at and below which the response is assumed to be constant and not different from the baseline rate of the controls. To achieve an accurate estimation of low concentration-responses, which is essential for the analysis and assessment of mixture effects, concentration-response models must be able to describe this threshold concentration, and data analysis should provide an accurate estimate of a threshold concentration from this model.

Together with the problem of baseline or spontaneous responses, the estimation of a threshold concentration defines a complex data and modelling situation which cannot be solved with classical concentration-response models. In the following we present threshold concentration-response models which we used for our data analysis, how these models were fitted to the data and how standard mixture models were adopted to our specific data situation.

Threshold dose-response models

The general equation of a threshold model with an implicit baseline response rate is given for a response likelihood p at concentration c by

$$P(c) = \begin{cases} F(\theta_1) & \text{for } c \le 10^d \\ F(\theta_1 + \theta_2 * (\log_{10}(c) - d)) & \text{for } c > 10^d \end{cases} \quad (2)$$

Here F(c) is a nonlinear concentration-response regression model from a family of continuous distributions, where θ_1 and θ_2 are location and scale model parameters. The threshold model parameter d defines the threshold concentration $c_{threshold}=10^d$, and the baseline rate of response is defined as $F(\theta_1)$.

We selected three potential models - logit, probit and weibull - all capable of accurately describing concentration-response data from the CBMN assay. The corresponding functions are

Logit: $$P(c) = \begin{cases} 1/\ 1+\exp(-\theta_1) & \text{for } c \le 10^d \\ 1/\ 1+\exp(-\theta_1 - \theta_2 * (\log_{10}(c) - d)) & \text{for } c > 10^d \end{cases} \quad (3)$$

Probit: $$P(c) = \begin{cases} \text{probnorm}(\theta_1) & \text{for } c \le 10^d \\ \text{probnorm}(\theta_1 + \theta_2 * (\log_{10}(c) - d)) & \text{for } c > 10^d \end{cases} \quad (4)$$

Weibull: $$P(c) = \begin{cases} 1-\exp(-\exp(\theta_1)) & \text{for } c \le 10^d \\ 1-\exp(-\exp(\theta_1 + \theta_2 * (\log_{10}(c) - d))) & \text{for } c > 10^d \end{cases} \quad (5)$$

Here probnorm(x) is the function that returns the probability that an observation from the standard normal distribution is less than or equal to x (inverse of the probit function).

All models were separately fitted to each data set, and then the best fitting model was selected for each chemical according to statistical criteria and used for the subsequent mixture modelling (Scholze et al. 2001). Only data from non-toxic concentrations were included in data analysis, and the IC_{40} earlier derived from a MTT assay was set as the upper limit above which toxicity was deemed to occur. Data analyses were always performed on pooled data sets from at least three independent experiments, and model parameters were estimated by (restricted) maximum likelihood. In some cases we observed a greater variability (statistical dispersion) in our data than was expected based on the binomial distribution, i.e. an extra binomial variation. In such cases we included an overdispersion parameter in the estimation process which was estimated from the Pearson statistic after all other parameters had been estimated.

Mixture predictions

For the prediction of mixture effects according to CA and IA, we adapted the two models to the use of threshold concentration-response relationships as described in the following.

Calculation of concentration addition

The concept of concentration addition is usually defined for a binary mixture of substances 1 and 2 by the equation

$$\frac{c_1}{ECx_1} + \frac{c_2}{ECx_2} = 1, \tag{6}$$

but can be extended to any number of n components by

$$\sum_{i=1}^{n} \frac{c_i}{ECx_i} = 1. \tag{7}$$

In these equations c_i are the individual concentrations of the substances 1 to n which are present in a mixture that produces the definite effect x, and ECx_i denotes the equivalent effect concentrations of the single substances, i.e. those concentrations that alone would produce the same quantitative effect x as the mixture. The individual concentrations c_i sum up to a total concentration c_{mix} that causes the joint effect $E(c_{mix}) = x$, and thus by definition is the effect concentration ECx_{mix}. Hence, c_i in Equation (7) can be substituted for the expression $p_i \bullet ECx_{mix}$, with p_i defined as the prevalence of a mixture component in the mixture, i.e. the ratio of its concentration to the total mixture concentration ($p_i = c_i / c_{mix}$). By rearrangement we then get:

$$ECx_{mix} = \left(\sum_{i=1}^{n} \frac{p_i}{ECx_i} \right)^{-1} . \tag{8}$$

The individual effect concentrations ECx_i are derived from individual concentration-response functions F_i. For that purpose the inverse functions F_i^{-1} are used, which give the concentrations c of the i^{th} substances that produce an individual effect x, i.e. $ECx_i = F_i^{-1}(x)$. Thus we can write:

$$ECx_{mix} = \left(\sum_{i=1}^{n} \frac{p_i}{F_i^{-1}(x)} \right)^{-1} . \tag{9}$$

An effect concentration derived from the threshold concentration-response model can only be estimated for effect levels above the baseline response, and is defined for the functions from Equations (3)-(5) as

Logit: $$F^{-1}(x) = 10^{\hat{d} - \frac{\log_e(1/(1-x))+\hat{\theta}_1}{\hat{\theta}_2}} \quad \text{for } x > 1/\ 1+\exp(-\hat{\theta}_1) \qquad (10)$$

Probit: $$F^{-1}(x) = 10^{\hat{d} + \frac{\text{probit}(x)-\hat{\theta}_1}{\hat{\theta}_2}} \quad \text{for } x > \text{probit}(\hat{\theta}_1) \qquad (11)$$

Weibull: $$F^{-1}(x) = 10^{\hat{d} + \frac{\log_e(-\log_e(1-x))-\hat{\theta}_1}{\hat{\theta}_2}} \quad \text{for } x > 1-\exp(-\exp(\hat{\theta}_1)) \qquad (12)$$

Here $\hat{\theta}_1, \hat{\theta}_2$ and $\hat{d}$ are estimates of the unknown model parameter θ_1, θ_2 and d, derived from the best-fitting approach.

Equation (9) allows the prediction of any effect concentration of a mixture under the hypothesis of concentration addition, however, only for effect levels x that are greater than the highest individual baseline rate from the individual compounds (because only in this case effect concentration calculations are possible for all compounds). The baseline response for the mixture experiment cannot be predicted according to this equation, but might be below the lowest predictable effect level, and in this case we suggest ignoring the effect restrictions in Equations (10)-(12) which then allows the estimation of concentrations for effect levels even below the baseline rate.

Calculation of independent action

The basic version of independent action has been formulated under the simple assumption that the susceptibilities of the individuals of an at-risk-population to different dissimilarly acting mixture components are not correlated with each other. For a binary mixture, this is commonly defined by the equation

$$E(c_{mixture}) = E(c_1) + E(c_2) - E(c_1) \bullet E(c_2) \quad . \tag{13}$$

$E(c_1)$ and $E(c_2)$ denote the effects produced by the individual compounds c_1 and c_2, and $E(c_{mixture})$ is the total effect of the mixture. This equation can be extended to any number of mixture components, resulting in

$$E(c_{mixture}) = 1 - \prod_{i=1}^{n} (1 - E(c_i)) . \tag{14}$$

The individual effects of mixture compounds $E(c_i)$ are calculated from concentration-response functions F_i determined for single substances, i.e. $E(c_i) = F_i\ (c_i)$. For concentration-response models with a baseline effect the single effects have to be first corrected by their individual background baseline estimates ($baseline_i$), and in the end the total mixture effect should be corrected by an estimate for the expected baseline for the mixture, i.e.

$$E(c_{mix}) = 1 + baseline_{mixture} - \prod_{i=1}^{n} (1 - (F_i(x) - baseline_i)) . \tag{15}$$

Ideally, all baseline estimates would be identical and thus work as a common reference. It is therefore important that the variation between the individual baseline estimates is reasonably small, which demands a good reproducibility of the test system and an experimental design that ensures accurate and precise estimations of all background baselines. If this is not the case, the estimation of a common baseline from all data must be implemented in the concentration-response data analysis of the compounds. There is no golden rule about how to estimate the baseline response for the mixture experiment. We used the smallest and highest baseline from all compounds and calculated for each mixture concentration two effect predictions, spanning a range of IA predictions.

Statistical uncertainty analyses for mixture response predictions and comparative assessment

For the effect endpoint in this project, CA and IA were used as empirical models to describe the mixture effects on the basis of the single compound information, and as such they were expected to approximate mixture responses only to a certain degree of certainty. In a strict qualitative sense, these models can never predict future mixture responses exactly, and a disagreement between observed and predicted mixture effects will always occur, however small and irrelevant they are, in the same way as a weather forecast can never predict an exact temperature. Therefore an empirical mixture assessment doesn't ask if, but how close mixture responses can be predicted. Traditionally a statistical test would formulate a null hypothesis about an exact agreement between the mean observed and predicted mixture response, and data would have the burden to reject this hypothesis. However, as the alternative hypothesis can be considered *a priori* as correct, consequently only a lack of statistical power would prevent the rejection of the null hypothesis (and thus accepting a disagreement between observed and predicted mixture responses). More appropriate would be a null hypothesis formulating a pre-defined maximal difference between observed and mixture responses as acceptable ("size of deviation is smaller than x"), and accepting only the alternative hypothesis ("disagreement") if the difference exceeds the pre-defined size according to statistics. This would require not only defining a minimal deviation that can be considered as small and irrelevant, but also the development of corresponding statistical test methods that would have to consider various threshold regression models and the mechanistic of the two given mixture models. Both are difficult, and to our knowledge such test methods don't exist.

We used an alternative statistical approach for assessing statistical significance by using the confidence intervals as interval estimates around the predicted and observed mean mixture responses: if the confidence intervals don't overlap we can conclude significance, and the deviation between the means provide information which than can be judged as relevant or not. Generally this approach is more conservative, i.e. if two confidence intervals overlap, the difference between the two means still may be significantly different. Mean estimations of effects and effect concentrations of individual substances are subject to a stochastic variability. As consequence, calculations of expected mixture responses according to Eqs. (9) and (15) also give a mean that is affected by statistical uncertainty. As a quantitative measure for this uncertainty we determined approximate 95% confidence intervals for mean predicted effects and effect concentrations by employing the bootstrap methodology (Efron and Tibshirani 1993): the bootstrap samples were generated on the basis of the effect distributions that were estimated within the fitting process for every individual concentration response function (parametric bootstrap), and used to generate a pool of resampled mixture predictions. The central 95% percentiles of this distribution were then used as approximation of the 95% interval estimates around the prediction. Finally, differences between predicted and observed effect concentrations were deemed statistically significant when the 95% confidence belts of the prediction did not overlap with those of the experimentally observed mixture effects. It should be noted that these intervals act as estimates of the unknown population mean (i.e. the mixture prediction), but not as an estimate of an interval in which future individual responses will fall. The latter would be achieved by so-called prediction intervals (or credible intervals in Bayesian statistics); however, both mixture models can predict only mean effect responses, but not individual response pattern.

Synergism or antagonism is present if deviations between observed and predicted mixture responses are judged as significant from a statistical and toxicological point of view. No formal decision criteria exist for the latter, but we considered a fivefold (or more) over- or underestimation of the observed effect concentrations as most relevant.

Mixture experiment design and testing

The concentration-response relationships of the CBMN positive benzimidazoles and non-benzimidazole compounds (Table 4) were used to design a set of mixtures to be tested in the CBMN assay. We chose a fixed mixture ratio approach (Altenburger et al. 2000) with mixture ratios proportional to equi-effective levels for all mixtures. To enhance the discrimination between the predictions from the two competing mixture models CA and IA, we used simulation studies to investigate which common effect level would be optimal to manifest the fixed-ratio mixture design. Based on these studies, we concluded that a mixture in which all components were combined in proportion to their estimated threshold concentrations would be an optimal solution. This further allowed us to investigate whether this combination of "zero" effect concentrations would produce a clear response. First, a mixture of the seven CBMN positive benzimidazoles was designed. The second mixture was composed of one selected benzimidazole (flubendazole) together with four non-benzimidazole aneugens. Mixture III consisted of flubendazole combined with the clastogens and mixture IV was a binary mixture of flubendazole and paclitaxel.

Flubendazole was chosen due to its potency and data reproducibility. We decided to test a mixture including clastogens to test for a broader variety of mechanisms of action. The binary mixture was chosen to investigate whether it is possible to perform a clear comparative mixture assessment with two compounds on the basis of the given data resources. This mixture included compounds with the same target (tubulin) but different binding sites and mechanisms of action (microtubule formation versus depolymerisation).

A summary of the mixture compositions and the mixture ratios is presented in Table 8.

All mixtures were designed in a similar way, i.e. components were combined in proportion to their estimated threshold concentrations. Mixture stocks at the defined mixture ratios were prepared and serially diluted to cover the predicted effective concentration range. Finally, the mixture effects were assessed experimentally in the CBMN assay and compared to the predictions.

Table 8: Composition of the four mixtures tested in the CBMN assay.
Percentages show the fraction of the individual compounds in the mixture.

Compound	Mixture I	Mixture II	Mixture III	Mixture IV
Albendazole	1.09%	-	-	-
Albendazole oxide	61.46%	-	-	-
Benomyl	19.17%	-	-	-
Carbendazim	15.26%	-	-	-
Flubendazole	0.78%	1.44%	34.77%	68.60%
Mebendazole	0.99%	-	-	-
Oxibendazole	1.25%	-	-	-
Colchicine	-	1.82%	-	-
Griseofulvin	-	96.07%	-	-
Vinblastine sulfate	-	0.01%	-	31.40%
Paclitaxel	-	0.66%	-	-
Mitomycin C	-	-	2.04%	-
Etoposide	-	-	8.89%	-
Melphalan	-	-	52.29%	-
Doxorubicin hydrochloride	-	-	2.01%	

References

Boobis AR, Daston GP, Preston RJ, Olin SS., 2009: *Application of key events analysis to chemical carcinogens and noncarcinogens.* Crit Rev Food Sci Nutr., 49(8):690-707.

Castelain, P., Van Hummelen, P., Deleener, A. and Kirsch-Volders, M. 1993: *Automated detection of cytochalasin-B blocked binucleated lymphocytes for scoring micronuclei.* Mutagenesis, 8, 285–293.

Committees on Toxicity, Mutagenicity and Carcinogenicity of Chemicals in Food, Consumer Products and the Environment, *Annual Report* 1993

Committees on Mutagenicity of Chemicals in Food, Consumer Products and the Environment, 2007: *Statement: Benzimidazoles: an approach to defining a common aneugenic grouping.* COM/07/S3 April 2007

Decordier, I., Papine A, Plas G, Roesems S, Vande Loock K, Moreno-Palomo J, Cemeli E, Anderson D, Fucic A, Marcos R, Soussaline F, Kirsch-Volders M. 2009: *Automated image analysis of cytokinesis-blocked micronuclei: an adapted protocol and a validated scoring procedure for biomonitoring.* Mutagenesis, 24, 85–93.

Drescher K, Boedeker W. 1995: *Assessment of the combined effects of substances: The relationship between concentration addition and independent action.* Biometrics 51:716–730.

Elhajouji A, Lukamowicz M, Cammerer Z, Kirsch-Volders M., 2011: *Potential thresholds for genotoxic effects by micronucleus scoring.* Mutagenesis, 26(1):199-204. Review.

Efron, B., Tibshirani, R.J., 1993: *An Introduction to the Bootstrap*. Chapman & Hall/CRC.

Faust M, Altenburger R, Backhaus T, Blanck H, Boedeker W, Gramatica P, Hamer V, Scholze M, Vighi M, Grimme LH, 2001: *Predicting the joint algal toxicity of multi-component s-triazine mixtures at low-effect concentrations of individual toxicants.* Aquat. Toxicol. 56, 13–32.

Kortenkamp A, Evans R, Faust M, Kalberlah F, Scholze M, Schuhmacher-Wolz U, 2012: *Investigation of the state of the science on combined actions of chemicals in food through dissimilar modes of action and proposal for science-based approach for performing related cumulative risk assessment,* SCIENTIFIC / TECHNICAL REPORT submitted to EFSA, http://www.efsa.europa.eu/en/supporting/doc/232e.pdf

Lynch A, Harvey J, Aylott M, Nicholas E, Burman M, Siddiqui A, Walker S, Rees R., 2003: *Investigations into the concept of a threshold for topoisomerase inhibitor-induced clastogenicity.* Mutagenesis, 18(4):345-53.

Mosmann, T. 1983: *Rapid colorimetric assay for cellular growth and survival: application to proliferation and cytotoxicity assays.* J. Immunol. Methods 16;65 (1–2), 55–63.

OECD, *In Vitro Mammalian Cell Micronucleus Test (MNvit), OECD Guideline for Testing of Chemicals No. 487*, OECD, Paris. Available at: http://www.oecd.org/env/testguidelines, 2010

Scholze, M., Boedeker, W., Faust, M., Backhaus, T., Altenburger, R., Grimme, L.H., 2001: *A general best-fit method for concentration–response curves and the estimation of low-effect concentrations*. Environ. Toxicol. Chem. 20, 448–457.

Varga, D., Johannes, T., Jainta, S., Schuster, S., Schwarz-Boeger, U., Kiechle, M., Patino Garcia, B. and Vogel, W. 2004: *An automated scoring procedure for the micronucleus test by image analysis.* Mutagenesis, 19, 391–397.